Functional characterization of aspartate aminotransferase from *Toxoplasma gondii*

2020

Jixu LI

Doctoral Program in Animal and Food Hygiene

Graduate School of Animal Husbandry

Obihiro University of Agriculture and Veterinary Medicine

トキソプラズマのアスパラギン酸アミノ基転移酵素の機能解析

令和 2 年

(2020)

帯広畜産大学大学院畜産学研究科

畜産衛生学専攻博士後期課程

李積旭

Contents

Abbreviations and unit abbreviations

Abbreviations

A	*AAT*	Aspartate aminotransferase gene
	Δaat	A mutant strain of deleted *AAT* gene in wild-type *T. gondii* parasite
	AlAAT	Alanine transaminase gene
	APAD	3-Acetylpyridine adenine dinucleotide
	APADH	3-(aminomethyl) cyclobutane-1-carboxylic acid hydrochloride
B	BSA	Bovine serum albumin
C	CAR	Carboxymethoxylamine
	Cas9	Clustered regularly interspaced short palindromic repeats-associated protein
	CCK8	Cell counting kit-8
	cDNA	Complementary deoxyribonucleic acid
	ComAAT	A complementary strain of *AAT* gene in *Δaat* parasite
	Ct	Cycle threshold values
	CRISPR	Clustered regularly interspaced short palindromic repeats
	CytB	*Toxoplasma* mitochondrial genome cytochrome b gene
D	DAPI	4',6-diamidino-2-phenylindole
	DDW	Double distilled water
	DHFR	Dihydrofolate reductase gene
	DMEM	Dulbecco's modified eagle’s medium
	DMSO	Dimethyl sulfoxide
	DNA	Deoxyribonucleic acid

	dpi	Day post-infection
E	EDTA	Ethylenediaminetetraacetic acid
	E. coli	*Escherichia coli*
	ELISA	Enzyme-linked immunosorbent assay
	EF-Tu	Apicoplast genome elongation factor Tu
	EMEM	Eagle's minimum essential medium
G	GABA	γ-aminobutyric acid
	GAPDH	Glyceraldehyde-3-phosphate dehydrogenase gene
	GDH	Glutamate dehydrogenase gene
	GFP	Green fluorescent protein
	GRAs	Dense granule organelles
	gRNA	Guide ribonucleic acid
	GST	Glutathione S-transferase
H	HFF	Human foreskin fibroblast
	HRP	Horseradish peroxidase
	HXGPRT	Hypoxanthine xanthine guanosine phosphoribosyl transferase gene
	HYD	Hydroxylamine
I	IC_{50}	Half maximal inhibitory concentration
	IFAT	Immunofluorescent antibody test
	IFN-γ	Interferon gamma
	IgG	Immunoglobulin G
	IL-10	Interleukin-10
	IL-12	Interleukin-12
	iNOS	Inducible nitric oxide synthase
	i.p.	Intraperitoneal injection

K	Km	Michaelis constant
L	LD_{50}	Median lethal dose
	LD_{100}	Absolute lethal dose
M	ME49	Low virulent *T. gondii* type II strain
N	NK	Natural killer cell
	NLS	Nuclear localization signal
P	PBS	Phosphate buffered saline
	PCR	Polymerase chain reaction
	PLK	Low virulent *T. gondii* type II strain
	Pru	Low virulent *T. gondii* type II strain
	PV	Parasitophorous vacuole
	PVM	Parasitophorous vacuole membrane
Q	qPCR	Quantitative real-time polymerase chain reaction
R	r	Recombinant
	RB	Enzyme activity test control group
	RH	Highly virulent *T. gondii* type I strain
	RNA	Ribonucleic acid
	RT	Room temperature
	RT-PCR	Reverse transcription polymerase chain reaction
S	SAGs	Surface antigens
	SDS-PAGE	Sodium dodecyl sulfate-polyacrylamide gel electrophoresis
	SI	Selectivity index
	SEM	Standard error of mean
T	TB	Enzyme activity test control group
	TCA	Tricarboxylic acid cycle

	Th1	T helper (Th1) cells
	TNF-α	Tumor necrosis factor alpha
U	*UPRT*	Uracil phosphoribosyl transferase gene
	UTR	Untranslated region
V	VEG	Avirulent *T. gondii* type III strain
	Vero	Monkey kidney adherent epithelial cell
	Vmax	Maximum reaction rate of enzymatic reaction
W	WB	Western blotting
	WT	Wild type

Unit abbreviations

bp	base pair
kb	kilo base
kDa	kilodalton
µl	microliter
ml	milliliter
ng	nanogram
µg	microgram
mM	millimolar
nM	nanomolar
nm	nanometre
s	second
min	minute
h	hour
U	unit
%	percentage

℃	degree Celsius

General introduction

1. *Toxoplasma gondii*

Toxoplasma gondii is an obligate intracellular parasite that belongs to the Apicomplexan protozoa, which is widely distributed throughout the world (Montoya and Liesenfeld, 2004; Weiss and Dubey, 2009; Saadatnia and Golkar, 2012). *T. gondii* is a very important food-borne zoonotic pathogen that can infect almost all warm-blooded animals, including humans (Montoya and Liesenfeld, 2004; Weiss and Dubey, 2009; Elmore et al., 2010; Saadatnia and Golkar, 2012). This pathogen can complete its life cycle in cats, the definitive host, by sexual reproduction and in humans or other intermediate hosts by asexual reproduction (Fig. 1) (Dubey, 1998, 2009a; Hunter and Sibley, 2012; Halonen and Weiss, 2013; VanWormer et al., 2013; Aguirre et al., 2019). There are various pathogenic forms that infect the hosts, fast-growing tachyzoites, slow-growing bradyzoites or cysts, oocysts, etc (Halonen and Weiss, 2013). Humans can be infected through ingestion of infectious oocysts or tissue cysts from food or water, and congenital infections through vertical transmission (Montoya and Liesenfeld, 2004; Dubey et al., 2005).

T. gondii lytic cycle starts with an energy-dependent extracellular tachyzoite invasion into host cells, which is followed by formation of the parasitophorous vacuole membrane (PVM). Parasites undergo several rounds of the lytic cycle following rapid intracellular tachyzoite replication, egress, and reinvasion of neighboring cells, a destructive process within the host cells can be observed by checking plaque formation *in vitro* (Fig. 2) (Black and Boothroyd, 2000). During a *T. gondii* infection, most of the fast-lytic tachyzoites can be transformed into the form

of slow-bradyzoites resulting in chronic infection (Matsubayashi and Akao, 1963; Soete et al., 1993).

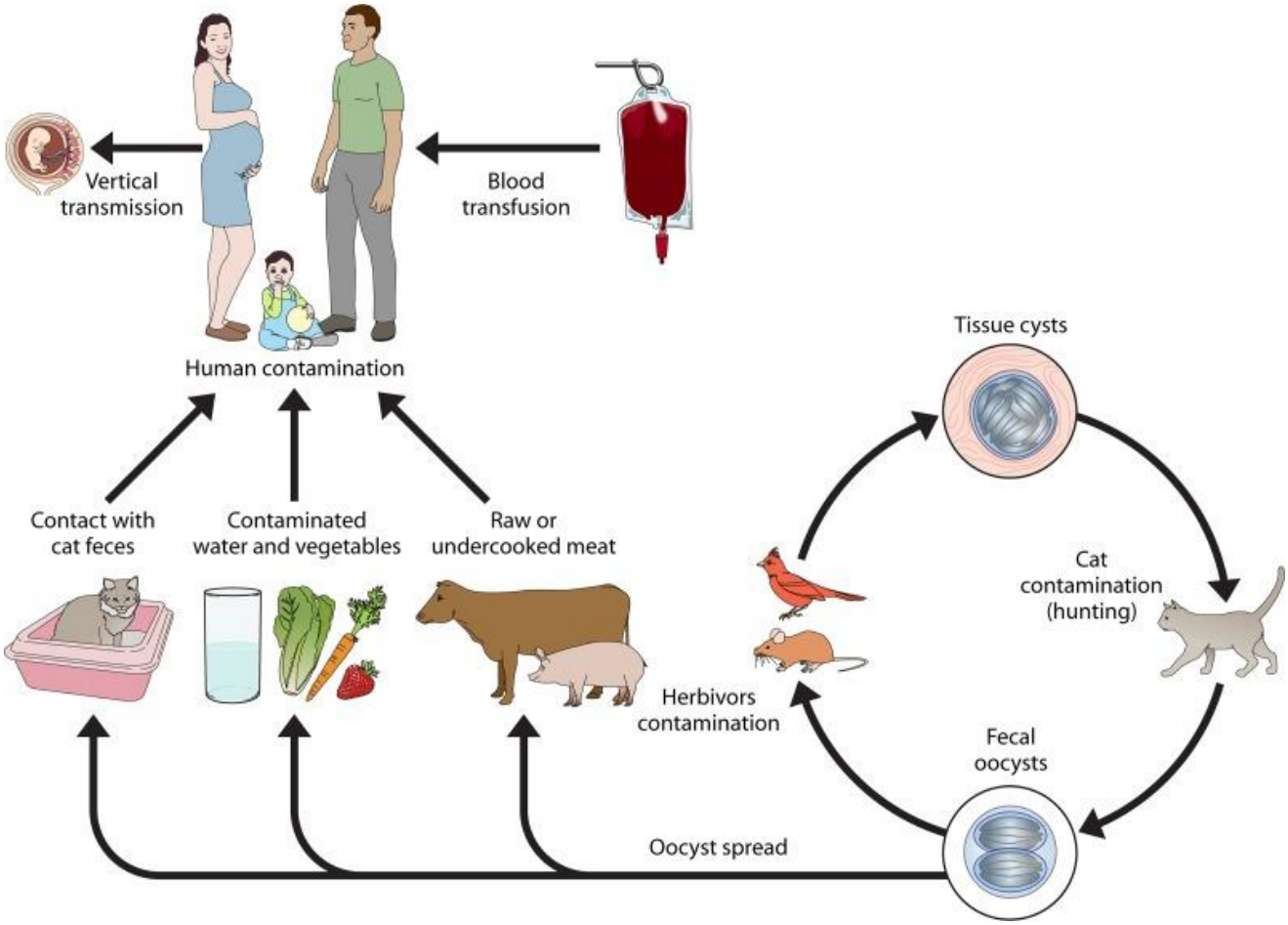

(Esch and Petersen et al., 2013)

Fig. 1. Life cycle of *T. gondii* and transmission in humans, domestic animals, wildlife and ecosystems.

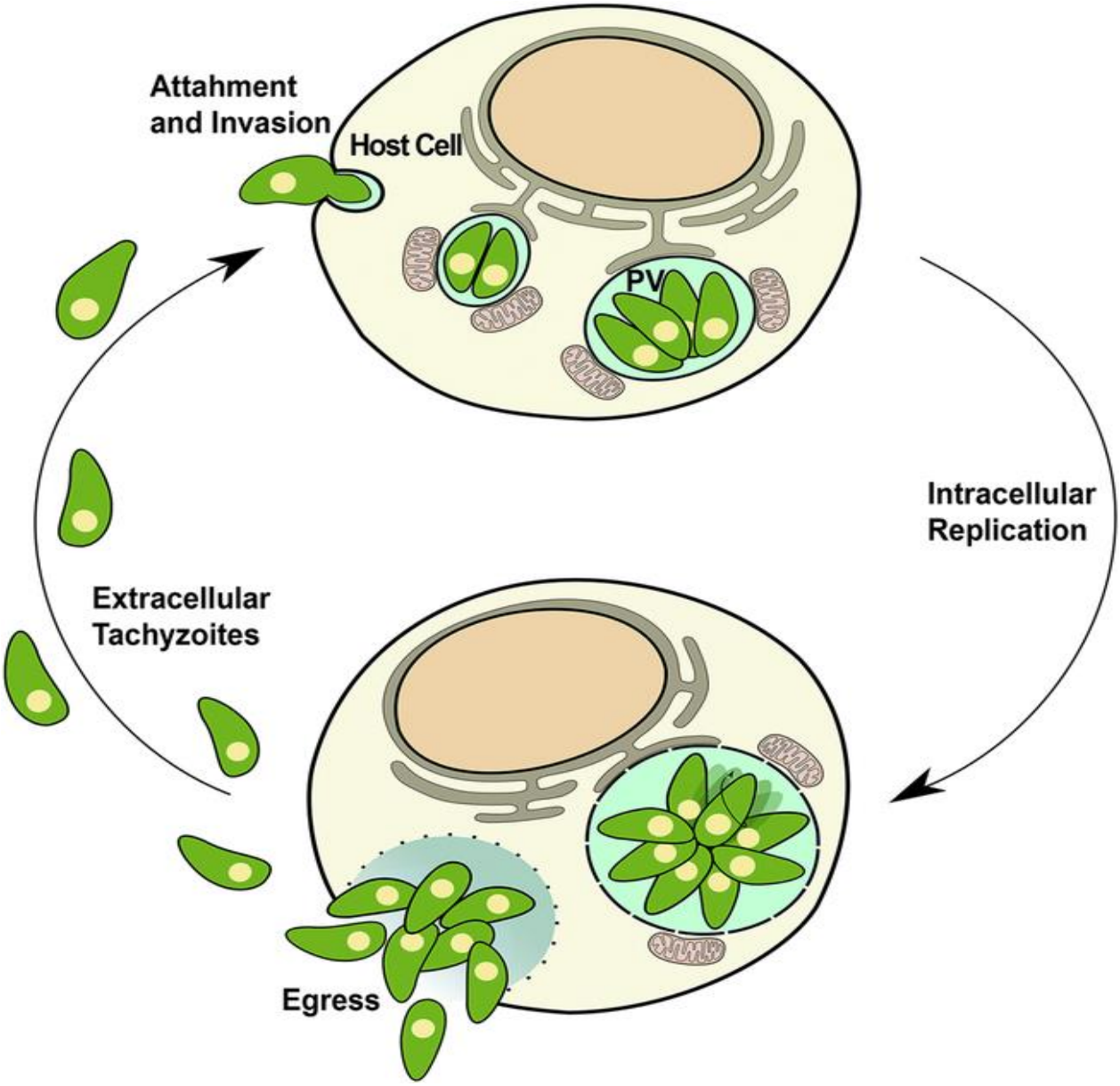

(Hortua Triana et al., 2018)

Fig. 2. The *T. gondii* lytic cycle. The five steps of *T. gondii* lytic cycle from extracellular tachyzoite invasion into host cells, to formation of PVM, rapid intracellular tachyzoite replication, egress, reinvasion of neighboring cells, and parasites undergoing several rounds of the lytic cycle.

2. Toxoplasmosis

Toxoplasmosis is a zoonotic parasitic disease caused by the obligate intracellular protozoan *T. gondii*. The disease threatens a range of warm-blooded mammals including humans. Toxoplasmosis has a worldwide distribution, and is very harmful to both human health and the livestock industry. It is reported that one-third of the population of the world is estimated to be infected with *T. gondii* (Halonen and Weiss, 2013; Wong et al., 2020), but the infection is usually asymptomatic in immunocompetent individuals, while immunocompromised people may acquire acute toxoplasmosis or even severe to fatal complications. In animal husbandry, toxoplasmosis caused by *T. gondii* infection is economically important in animals, such as pigs and sheep. The infection leads to abortion or stillbirth, reduction in quality of milk, meat or other animal products, resulting in huge economic losses. Moreover, there is a risk of transmitting the infection to humans through the consumption of contaminated animal products (Montoya and Liesenfeld, 2004; Dubey et al., 2005; Dubey, 2009b).

T. gondii infection causes varying degrees of threat to the hosts, the development of acute or chronic toxoplasmosis, mainly depends on the pathogenicity of the different *T. gondii* strains. In a mouse model, early research found that the genotypes of *T. gondii* causing toxoplasmosis in North America and Europe are mainly divided into classes I, II, and III (Howe and Sibley, 1995; Khan et al., 2011). The difference between these three types of *T. gondii* is the virulence, that is to say, the type I strains are the most virulent (RH strain, $LD_{100} \geq 1$ tachyzoite), type II strains are moderately virulent (ME49, PLK, and Pru strains, $LD_{50} = 10^3$-10^5 tachyzoites), and type III strains are the weakly virulent (VEG strain, usually 10^5 tachyzoites in mice are also

rarely killed) (Howe and Sibley, 1995; Khan et al., 2011). These studies have shown that there are differences in the virulence or pathogenicity of clinical isolates with different genotypes in the mouse model. Human infection with different genotypes of *T. gondii* can also show varying degrees of disease from mild toxoplasmosis which can be asymptomatic or present with mild flu-like symptoms to severe or acute toxoplasmosis or even death. The infection may be even become chronic infection leaving the patient a long-term carrier of this parasite.

3. Treatment of toxoplasmosis

To develop effective treatment for *T. gondii* infection, key enzymes, involved in metabolism, growth, synthesis of essential substances or virulence, are considered as an ideal target, and inhibitors (small molecular compounds) of these enzymes have been discovered as an effort towards control of toxoplasmosis (Cowell and Winzeler, 2019; Wang et al., 2019a). Drugs like pyrimethamine, which inhibit dihydrofolate reductase, an important enzyme in DNA synthesis of *T. gondii*, have been approved for treatment of toxoplasmosis (Brun-Pascaud et al., 1996; Lapinskas and Ben-Harari, 2019). Sulfadiazine (another approved drug), inhibits dihydrofolic acid synthetase which is a key enzyme in the synthesis of purines (Dantas-Leite et al., 2004; Salin et al., 2020). Recently, a combination of pyrimethamine and sulfadiazine or other compounds has been used to treat active toxoplasmosis in animals or humans (Alday and Doggett, 2017; Dunay et al., 2018). The limitations to the efficacy of this combination are the severe side effects, adverse drug reactions, and limited or no significant therapeutic efficiency on the bradyzoites. Therefore, these limit the effectiveness of toxoplasmosis treatment (Wei et al., 2015; Dunay et al., 2018).

On the other hand, in addition to the current unsatisfactory status in drug treatment of toxoplasmosis, there is the inability of eliminating tissue cysts within the host. There is an urgent need to identify ideal targets and develop the compounds which not only treat acute but also chronic toxoplasmosis. In this case, calcium-dependent protein kinase 1, plays an important role in the development of acute or chronic *T. gondii* infection in animals, for this reason, it has identified as potentially one of the most promising therapeutic targets towards the control of both acute and chronic toxoplasmosis (Lourido et al., 2010; Johnson et al., 2012; Cardew wt al., 2018; Lapinskas and Ben-Harari, 2019).

Recently, studies have shown that both innate and adaptive immune responses show a important role during controlling *T. gondii* infection (Pifer and Yarovinsky, 2011; Hunter and Sibley, 2012; Yarovinsky, 2014; Sasai et al., 2018; Lima and Lodoen, 2019; Sasai and Yamamoto, 2019), and that full protective immunity of host against its infection is a combination of both cellular and humoral immunity (Sayles et al., 2000; Spellberg and Edwards, 2001; Pifer and Yarovinsky, 2011; Xia et al., 2018b; Yang et al., 2019; Liang et al., 2020). Therefore, focus on immune response studies such as screening of the IFN-γ-dependent inhibitors of the growth of *T. gondii*, have become the basis for designing effective toxoplasmosis treatment strategies (Radke et al., 2018).

With the advent of the genomic era, the widespread application of the CRISPR/Cas9 system has permitted precise and efficient genetic manipulations in *T. gondii*. Manipulations: such as gene editing and gene deletion result in the development of gene-point mutations which can be easy selection and search for the active sites or targets of selected compounds (Shen et al., 2017). Hence, the screening of potential drug candidates for anti-*T. gondii* using CRISPR/Cas9 system and small

molecule compound synthesis has been developed. Most drug screening studies have targeted key enzymes of *T. gondii*, such as uracil phosphoribosyltransferase and adenosine kinase (Salin et al., 2020). In recent years, some compounds isolated from plants or bacteria have also been used to design and identify novel treatments for toxoplasmosis (Dittmar et al., 2016; Leesombun et al., 2016; McFarland et al., 2016; Alday and Doggett, 2017; Montazeri et al., 2017; Montazeri et al., 2018a; Adeyemi et al., 2019; Deng et al., 2019; Wang et al., 2019a). Although these compounds have achieved significant effects *in vitro* and *in vivo*, no clear targets of drug actions confirmed and these compounds have not been used clinically.

Overall, although the public health problems and agricultural economic losses caused by *T. gondii* infections are known worldwide, the challenges to control *T. gondii* infection and treat toxoplasmosis have been arduous, not only because of the complex life cycles and multiple routes of transmission, but also because of the diverse population of *T. gondii* strains. To date, safe and effective drug treatment against toxoplasmosis remains a challenge. Therefore, the search for and development of effective and safe drug treatments controling toxoplasmosis in humans and animals is needed.

4. Aim of the present study

The CRISPR-Cas9 editing system in *T. gondii* has been widely used in type I RH and type II ME49 and PLK or other strains. This system can efficiently and accurately perform genetic operations, such as gene knockout, complementary, and mutation. Metabolic enzymes play crucial roles in growth and development of *T. gondii* parasites, so these enzymes can be used as potential drug targets for designing

toxoplasmosis treatment. Hence, in order to develop safer and more effective therapeutic drugs, CRISPR-Cas9 editing system was used to find a drug target in this study, and further assess the inhibitory effects of selected compounds *in vitro* or *in vivo*.

The objectives of this study are as follows: (1) to sequence the aspartate aminotransferase (*AAT*) genes both in *T. gondii* type I RH and type II PLK strains, and then to assess the enzyme activity; (2) to perform the functional analysis of AAT in both *T. gondii* type I RH and type II PLK strains using the CRISPR/Cas9 gene-editing system; (3) to evaluate the potential of *AAT* as a drug target, and determine the inhibitory effects of hydroxylamine (HYD) and carboxymethoxylamine (CAR) on *T. gondii in vitro* and *in vivo*.

Chapter 1

Characterization of aspartate aminotransferase of *Toxoplasma gondii*

1-1. Introduction

The phylum Apicomplexa comprises a grand group of intracellular parasites that have been implicated in many important human and veterinary diseases. The *Plasmodium* spp. and *Toxoplasma gondii* are the most representative and best studied members of this large phylum (Jacot et al., 2016). *T. gondii* is an obligate intracellular protozoan parasite which causes toxoplasmosis in warm-blooded animals, including humans (El Mouhawass et al., 2020). Majority of the isolates from North America and Europe belong to one of three distinct lineages based on the laboratory mouse model: acutely virulent type I strains, while intermediate type II, and avirulent type III (Howe and Sibley, 1995; Sibley and Ajioka, 2008; Guo et al., 2019). One-third of the population of the world is estimated to be infected with *T. gondii* (Halonen and Weiss, 2013; Wong et al., 2020), but the infection is usually asymptomatic in immunocompetent individuals, while immunocompromised people may be occur acute toxoplasmosis or even be severe complications to fatal. Unfortunately, although the gold-standard medicine for treating toxoplasmosis uses a combination of sulfonamide and pyrimethamine drugs (Leesombun et al., 2016), treatments for *T. gondii* infections are suboptimal (Wei et al., 2015; Scheele et al., 2018), as synergistic activity could only be observed against tachyzoites but not against bradyzoites, and severe side effects and adverse drug reaction are reported.

Metabolic enzymes play crucial roles not only in parasite proliferation but also in pathogenicity, which contribute to the virulence of parasites in mice models and used as potential drug targets (MacRae et al., 2012; Oppenheim et al., 2014; Zheng et al., 2015; Xia et al., 2018a; Xia et al., 2019). *T. gondii* genome contains only enzyme, the aspartate aminotransferase (*AAT*), as in *Plasmodium*, which catalyzes the reversible of conversion of oxaloacetate and glutamate to aspartate and α-ketoglutarate (Wrenger et al., 2011; Wrenger et al., 2012; Jacot et al., 2016). Here, the characterization of the predicted *AAT* genes was performed both in *T. gondii* type I RH and type II PLK strains to assess its enzyme activity and further evaluate the potential which could be used as a drug target.

1-2. Materials and methods

Animals

Female ICR and BALB/c mice with a six-week-old were purchased from the Clea Japan to generate the polyclonal antibodies targeting specific proteins in *T. gondii*. These experimental mice were maintained in the animal facility in the National Research Center for Protozoan Diseases, Obihiro University of Agriculture and Veterinary Medicine with adequate temperature (25±2℃) and luminosity (12-h light, 12-h dark), under specific pathogen-free conditions, and free access to food and water. All animal experiments started one week after habituation. This study strictly followed the recommendations of the Guide for the Care and Use of Laboratory Animals of Obihiro University of Agriculture and Veterinary Medicine, Japan. The current protocol was approved by the Committee on the Ethics of Animal

Experiments of Obihiro University of Agriculture and Veterinary Medicine, Japan (permission number: 201711).

Parasites culture

T. gondii hypoxanthine-xanthine-guanine phosphoribosyl transferase (*HXGPRT*) deleted-RH strain (type I), and PLK strain (type II) were used in this study. The parasites were cultured in monkey kidney adherent epithelial (Vero) cells cultured in Eagle's minimum essential medium (EMEM) (Sigma, USA) with 8% fetal bovine serum (FBS, Biowest, Japan), 100 U ml^{-1} penicillin and 100 mg ml^{-1} streptomycin (PS, Sigma, USA) at 37℃ and 5% CO_2, as described previously (Guo at al., 2019). To purify *T. gondii* tachyzoites, the host cells with the parasites were washed with sterile phosphate-buffered saline (PBS) and peeled from the plate with a cell scraper (BD Bioscience, USA). Then parasites were counted after passing through the 27-gauge needle syringe and filtering through the 5.0-μm pore filter (Millipore, USA). All procedures of pathogen experiments were carried out following with the guidelines of Obihiro University of Agriculture and Veterinary Medicine (permission number: 2018728).

Chemicals

Hydroxylamine (HYD) and carboxymethoxylamine hemihydrochloride (CAR) known as inhibitors of *AAT* were purchased from Sigma (catalog no. 7803-49-8 and 86-08-8). The inhibitors were dissolved in double distilled water (DDW) and dimethyl sulfoxide (DMSO), respectively, and stored at -30℃ until use.

Sequencing analysis

The *TgAAT* genes of RH strain (*Toxoplasma* Genomics Resource TGGT1_248600) and PLK strain (*Toxoplasma* Genomics Resource TGME49_248600) were amplified

by PCR from cDNA of *T. gondii* RH and PLK parasites, respectively. Primers include the forward primer 5'-ACGC GTCGAC ATG TTT CCA ACT CTT AGT GAG AAC C-3' and the reverse primer 5'-ATAAG*AAT* GCGGCCGC TTA GCT TGC AGG AAC TGC CCG CAC CA-3' were used. The PCR products were purified using QIAquick Gel Extraction Kit (QIAGEN, Germany) and cloned into *Escherichia coli* DH5α using the pGEM-T Easy Vector System (Promega, USA). Then the Dye Terminator Cycle Sequencing Kit (Applied Biosystems, USA) were used to do sequencing analysis of the positive clones using an ABI PRISM 3100 Genetic Analyzer (Applied Biosystems, USA). The obtained positive sequences were developed the BLASTn search analysis. The phylogenetic tree based on *AAT* genes was constructed using obtained *TgAAT*s sequences of RH and PLK compared with *AAT*s from other species using MEGA7: Molecular Evolutionary Genetics Analysis version 7.0 for bigger datasets (Kumar et al., 2016).

Production of recombinant proteins and polyclonal antibodies

The *TgAAT* genes of RH and PLK strain were amplified by PCR from cDNA of *T. gondii* RH and PLK parasites, respectively. Primers used included a *Sal* I site (underlined) in the forward primer 5'-ACGC GTCGAC ATG TTT CCA ACT CTT AGT GAG AAC C-3' and an *Not* I site (underlined) in the reverse primer 5'-ATAAG*AAT* GCGGCCGC TTA GCT TGC AGG AAC TGC CCG CAC CA-3'. The PCR products digested with *Sal* I and *Not* I, were inserted into the pGEX-4T-1 plasmid vector treated with the same restriction enzymes (Roche, Switzerland). The fragments were sequenced and checked by using Big Dye Terminator Cycle Sequencing Kit (Applied Biosystems, USA) in ABI PRISM 3100 Genetic Analyzer (Applied Biosystems, USA), as described previously (Guo at al., 2019). On the other hand, the pGEX-4T-3-SAG1 (Kimbita et al., 2001) and pGEX-4T-3-GRA7 (Masatani

et al., 2013) plasmids were used to produce recombinant *Tg*SAG1-GST and *Tg*GRA7-GST proteins. Recombinant pGEX-4T-1-AAT, pGEX-4T-3-SAG1 and pGEX-4T-3-GRA7 were expressed in *E. coli* BL21 (DE3) (New England BioLabs, USA) with glutathione S-transferase (GST) fusion protein and purified by using the Glutathione Sepharose 4B beads (GE Healthcare Life Sciences, USA), according to the manufacturer's instructions. Purified recombinant protein *Tg*AAT-GST (100 μg) and *Tg*SAG1-GST (100 μg) emulsified in the Freund's complete adjuvant (Sigma, USA) were intraperitoneally injected (i.p.) into BALB/c mice to induce *T. gondii* specific polyclonal antibodies of mouse anti-*Tg*AAT and anti-*Tg*SAG1. Meanwhile, the purified recombinant proteins of *Tg*SAG1-GST (1 mg) and *Tg*GRA7-GST (1 mg) were subcutaneously injected into the female Japanese white rabbits to prepare rabbit anti-*Tg*SAG1 and anti-*Tg*GRA7 polyclonal antibodies, as described previously (Guo at al., 2019).

Western blot analysis

In this study, these concentrations of all protein samples were confirmed by Pierce™ BCA Protein Assay Kit (Thermo Scientific, USA), and then SDS-PAGE and Western blot analysis were developed. The anti-AAT, anti-SAG1 and anti-GRA7 sera were used as primary antibodies. The goat anti-mouse or anti-rabbit immunoglobulin G (IgG) conjugated Horseradish peroxidase (HRP) (Amersham Pharmacia Biotech, USA) was used to be the secondary antibody to develop the reaction and measure the results by the VersaDoc™ imaging system (Nippon Bio-Rad Laboratories, Japan).

Enzyme activity assay

Enzyme-coupled assay were performed as described previously (Wrenger et al., 2011), and shown as Fig. 3 and Table 1. The concentration of soluble r*Tg*AAT-fused

GST was determined as 1 μg, which was used to process enzyme-coupled assay with specific substrate L-aspartate and α-ketoglutarate (Sigma, USA). The basic reaction principle is that L-aspartate and α-ketoglutarate were catalyzed to glutamate by r*Tg*AAT, then glutamate with 3-Acetylpyridine adenine dinucleotide (APAD, Sigma, USA) are converted to APADH by Glutamate Dehydrogenase (GDH, Sigma, USA), which the absorbance of supernatant was determined at 363 nm. Two reported specific enzymatic inhibitors including HYD and CAR (Sigma, USA) were used to determine inhibitors assay (Wrenger et al., 2011). All experiments were tested 3 times independently, and single GST was used as control.

Statistical analysis

The GraphPad Prism 7 software (GraphPad Software Inc., USA) was used to graph and analyze the data. Statistical analyses were performed in this study by using an unpaired Student's *t*-test analysis. Data represent the mean ± Standard Error of Mean. A p value < 0.05 was considered statistically significant (* $p < 0.05$, ** $p < 0.01$, *** $p < 0.001$ or **** $p < 0.0001$).

1-3. Results

Characterization of aspartate aminotransferase in *T. gondii* type I RH and type II PLK strains

In this study, the gene encoding *TgAAT* from the *Tg* type I RH and type II PLK strains were amplified and sequenced, indicating *TgAAT*s sequences were 1,794 bp long and coding 597 amino acid sequences. The *TgAAT*s sequence, amino acid sequence alignment was analyzed, and the phylogenetic tree was constructed with *AAT*s from other species including *Homo sapiens* (AAC28622.1), *Mus musculus*

(NP_034454.2), *Plasmodium falciparum* (KNG76684.1), *Babeisa microti* (XP_012650011.1), *Eimeria tenella* (XP_013230025.1), *Trypanosoma brucei* (AAK73815.1), *Giardia intestinalis* (AAK73817.1) and *Escherichia coli* (AHG10759.1) (Fig. 4A and B). It revealed that although they contain several conserved sequences in *AAT*s, *TgAAT*s were distantly related to the predicted *Homo sapiens* with 46%, *Mus musculus* with 46%, *P. falciparum* with 33% and *Neospora caninum* with 75% identities. Meanwhile, compared the sequences between RH and PLK, although six different amino acids of the sequences were found in two strains (Fig. 5A), the Western blot analysis revealed that the expression levels of native AAT protein in RH and PLK strains was not significantly different (Fig. 5B and C), suggests *Tg*AAT may play a similar role in both strains.

Enzyme activity of r*Tg*AAT

To determine the enzyme activity of rAAT from *Toxoplasma*, the soluble r*Tg*RHAAT and r*Tg*PLKAAT were expressed (Fig. 6A) and used to generate the enzyme-coupled assay as described previously (Fig. 2 and Table 1) (Wrenger et al., 2011). Soluble r*Tg*AAT (1 μg) was used to conduct enzyme reaction with specific substrate L-aspartate. The results showed that L-aspartate is the preferred substrate of both r*Tg*AATs (Fig. 6B, C and D). Meanwhile, the enzyme kinetic parameters were determined both two AATs from RH and PLK strains using increasing concentration of L-aspartate. The results showed that although there was no significant difference, the Vmax and Km values of r*Tg*PLKAAT were higher than r*Tg*RHAAT protein (Fig. 6E), which were consistent with that native AAT expression in PLK parasites was slightly higher than that the level in RH parasites. Furthermore, as expected, the reaction of 1 μg r*Tg*AAT was inhibited by HYD and CAR treatment with the 50% inhibitory concentration value of 0.4158 and 0.0035 μg/ml, respectively (Fig. 6F).

1-4. Discussion

In this study, *AAT* genes from *T. gondii* type I RH and type II PLK strains were amplified and sequenced. The results show that *TgAAT*s contain the 1,794 bp long nucleotide coding 597 amino acid sequences, and are single copies both in two different strains, which are consistent with the predicted sequences (ToxoDB: TGGT1_248600 and TGME49_248600). Compared with two *AAT* genes from RH and PLK sequences, it found that there are six different amino acids, however, this did not result in a significant difference in their expression levels in native parasites. This result suggests that AAT plays at least a similar role in RH and PLK strains. Importantly, the further determination of enzyme activity of r*Tg*RHAAT and r*Tg*PLKAAT proved the speculation, that they both could use the L-aspartate as a substrate to catalyze the reaction to produce glutamate without significant difference of activity, which is also consistent with the function of this enzyme in other parasites (Berger et al., 2001; Wrenger et al., 2011; Wrenger et al., 2012; Manchola et al., 2018).

Some enzymes from parasites have been characterized and identified to develop novel targets for chemotherapy in recent studies, and their inhibitors were widely used to control parasite infection (Müller and Hemphill, 2016; Montazeri et al., 2018b; Siqueira-Neto et al., 2018; Xie et al., 2019). Hence, in this present study, two compounds were tested in enzyme activity of r*Tg*RHAAT and r*Tg*PLKAAT, that of two inhibitors of AATs, namely HYD and CAR, abolished the transamination activity of r*Pf*AAT (Wrenger et al., 2011; Wrenger et al., 2012). As expected, HYD and CAR also significantly inhibited the transamination activity of r*Tg*AAT. Importantly, although the enzyme activity of AATs from human and mouse did not determine in

this study, the distant relationship of identities with humans and mice was found in *TgAAT* sequences from RH and PLK. These led me to consider whether *AAT* can be used as a key drug target and whether these two inhibitors can also specifically inhibit the growth of *T. gondii* without affecting the host, which needs to be proved by the next experiment.

1-5. Summary

In summary, a gene, *AAT*, was sequenced and characterized in *T. gondii* type I RH and type II PLK strains. Meanwhile, the ability of r*Tg*AAT for using the L-aspartate as a substrate was investigated, which is consistent with my predictions and the results in AAT activity from *Plasmodium*. Importantly, two reported inhibitors were further tested and found that they could indeed inhibit the activity of this enzyme (r*Tg*RHAAT and r*Tg*PLKAAT). Therefore, it is possible that these two drugs could also inhibit the growth of *T. gondii* to control toxoplasmosis and may through the pathway of *TgAAT*, but it remains to be proved by further experiments.

Table 1. Enzyme-coupled assay.

Reagents	Amount of addition			
	Enzyme	GST	TB	RB
r*Tg*RH/PLKAAT-GST	1 μg	--	1 μg	--
GST	--	1 μg	--	--
L-Aspartate	10 mM	10 mM	--	--
α-ketoglutarate	20 mM	20 mM	--	--
1 M Tris-HCl (PH8.0)	50 mM	50 mM	50 mM	50 mM
300 μl, mix, 37℃ for 30 min, boiling the samples for 1 min stop the enzymatic reaction				
APAD	0.5 mM	0.5 mM	0.5 mM	0.5 mM
Glutamate dehydrogenase	7 U	7 U	7 U	7 U
50 mM Tris-HCl (PH8.0)	50 mM	50 mM	50 mM	50 mM
The final volume of 1 ml, mix, 37℃ for 1 h, 14000g for 1 min, the absorbance of supernatant was determined at 363 nm				

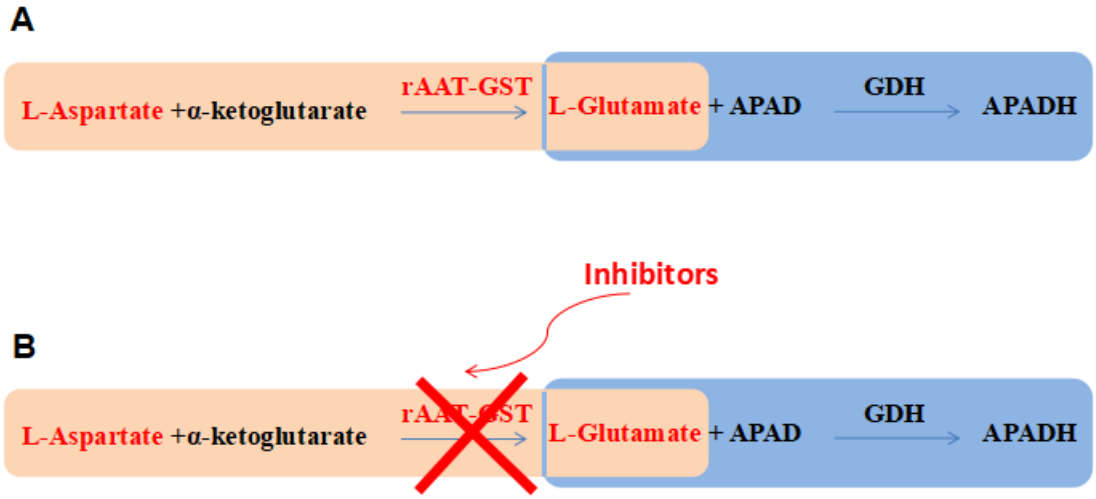

Fig. 3. Schematic diagram of enzyme activity (A) and inhibitory assay (B) of the r*Tg*AAT.

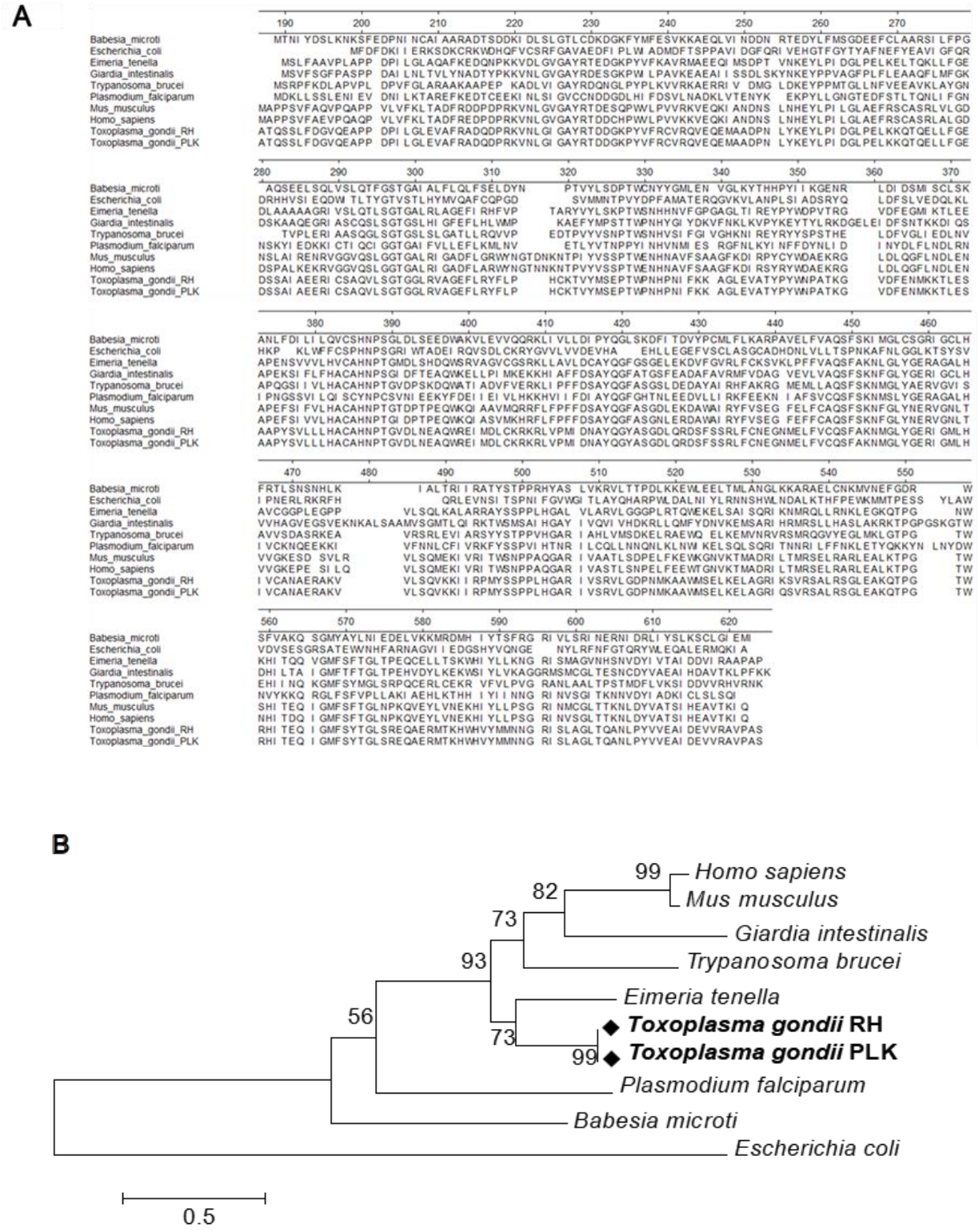

Fig. 4. Analysis of *AAT*s in different species. (A) Amino acid sequence analysis of *TgAAT* in type I RH and type II PLK strains (ToxoDB: TGGT1_248600 and

TGME49_248600) compared with *AAT*s from other species including *Homo sapiens* (AAC28622.1), *Mus musculus* (NP_034454.2), *Plasmodium falciparum* (KNG76684.1), *Babeisa microti* (XP_012650011.1), *Eimeria tenella* (XP_013230025.1), *Trypanosoma brucei* (AAK73815.1), *Giardia intestinalis* (AAK73817.1) and *Escherichia coli* (AHG10759.1). (B) Phylogenetic tree of *AAT*s from different species.

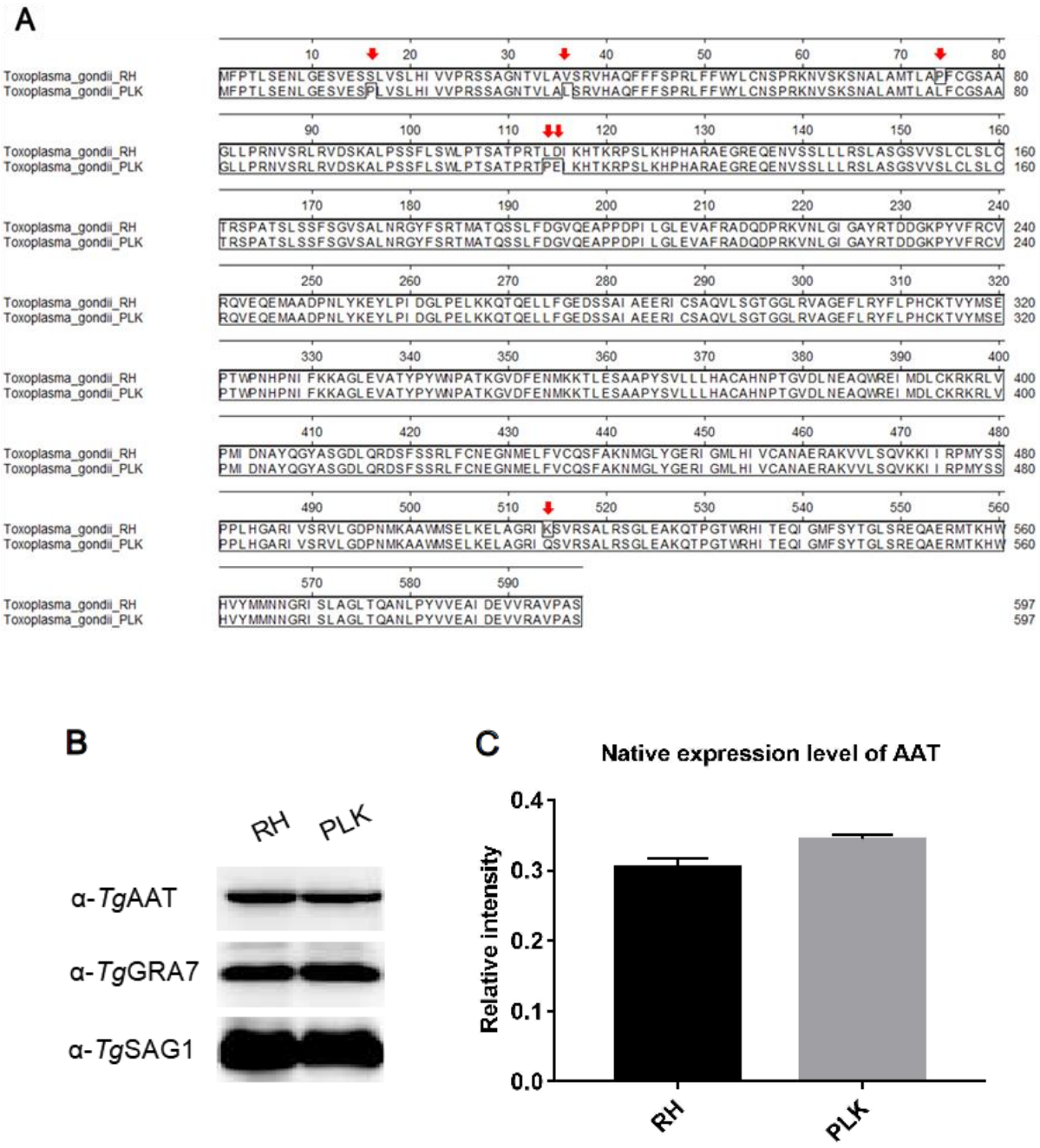

Fig. 5. Analysis of *AATs* in *T. gondii*. (A) Sequence analysis of *TgAAT* between type I RH and type II PLK strains. (B and C) Expression levels of native AAT protein in RH and PLK strains. Means ± SEM of three independent experiments are shown, unpaired Student's *t*-test.

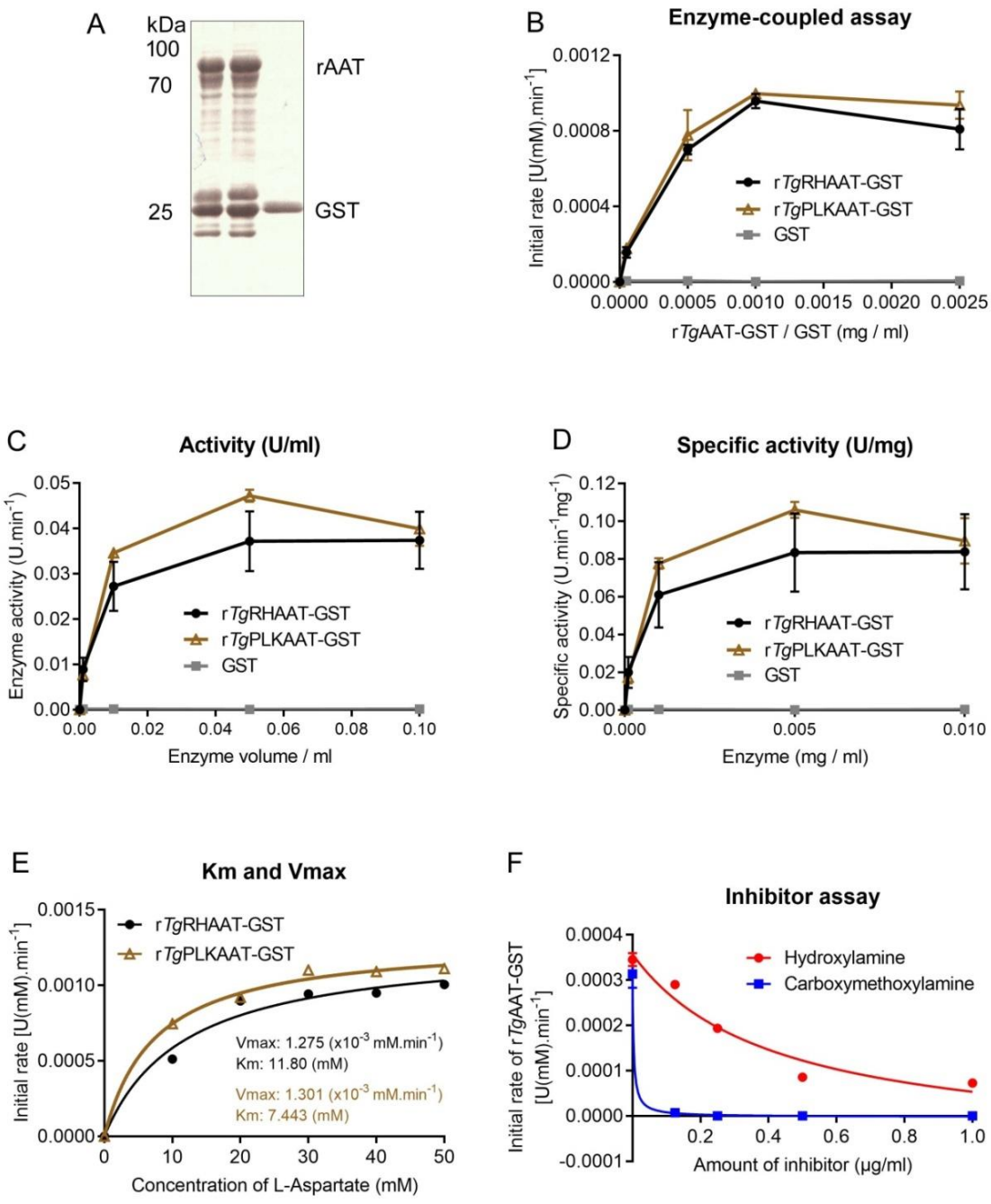

Fig. 6. Analysis of enzyme activity of r*Tg*AAT. (A) Soluble r*Tg*RH/PLKAAT protein expressions. The concentration of soluble r*Tg*AAT-fused GST was determined. (B) Generation of enzyme-coupled assay. Expressed GST was used as a control. (C, D and E) Enzyme reaction. Enzyme activity of catalysis aspartate and α-ketoglutarate

into glutamate was determined using 1 μg r*Tg*AAT. The enzyme activity, specific activity and enzyme kinetic parameters were determined both two rAATs from RH and PLK strains. (F) Inhibitor assay. Enzyme reaction was inhibited with increasing amount of Hydroxylamine (HYD) and Carboxymethoxylamine (CAR).

Chapter 2

Functional analysis of aspartate aminotransferase from *Toxoplasma gondii in vitro* and *in vivo*

2-1. Introduction

Toxoplasma gondii lytic cycle develops to start from the extracellular tachyzoite invasion with energy-dependent into host cells, then that is followed by rapid intracellular tachyzoite replication, egress, and reinvasion of neighboring cells (Nitzsche et al., 2016). In these stages, not only glucose, but also glutamine can enter the mitochondria as carbon source (Fleige et al., 2007; Fleige et al., 2008; MacRae et al., 2012; Blume et al., 2015; Nitzsche et al., 2016), wherein glutamine can be utilized as carbon skeletons to the tricarboxylic acid cycle (TCA cycle) via either the conversion of intermediate glutamate to α-ketoglutarate or the γ-aminobutyric acid (GABA) shunt (MacRae et al., 2012). *T. gondii* genome contains enzymes allowing speculation on a possible architecture of α-ketoglutarate pathway (Jacot et al., 2016), which includes an aspartate aminotransferase (*AAT*). AAT, as metabolic enzyme, catalyzes the reversible of conversion of oxaloacetate and glutamate into aspartate and α-ketoglutarate, and subsequently α-ketoglutarate as an intermediate can entry into the TCA cycle used for *T. gondii* proliferation (Jacot et al., 2016). Hence, this study focused on the pathway of the conversion intermediate glutamate to α-ketoglutarate in glutaminolysis related to *AAT*, and performed the functional analysis of the predicted *AAT* genes of these in both *T. gondii* type I RH and type II PLK strains using the CRISPR/Cas9 gene-editing system.

2-2. Materials and methods

Animals

Female BALB/c mice with a six-week-old were purchased from the Clea Japan for survival assay. Mice were maintained in the animal facility under specific pathogen-free conditions, and free access to food and water, as described above. All animal experiments started one week after habituation. All animal and pathogen experiments have strictly followed the Committee on the Ethics of Animal Experiments or Pathogen Experiments of Obihiro University of Agriculture and Veterinary Medicine, Japan, as described above.

Parasites culture

T. gondii type I hypoxanthine-xanthine-guanine phosphoribosyl transferase (*HXGPRT*) deleted-RH strain and type II PLK strain were used in this study. The Vero cells cultured in EMEM were used to maintain *T. gondii*, as described above. Meanwhile, the parasites were maintained in human foreskin fibroblast (HFF) cells cultured using Dulbecco's modified Eagle's medium (DMEM, Sigma) supplemented with 10% FBS, as well as 100 U ml^{-1} penicillin and 100 mg ml^{-1} streptomycin in a 5% CO_2 atmosphere of 37 ℃. For the purification of tachyzoites, a cell scraper, 27-gauge needle and 5.0-μm pore filter were used as described above.

Knockout *AAT* gene on RH and PLK strains

All the primers used in the present study are listed and showed in Table 2. *T. gondii* aspartate aminotransferase-targeting guide RNA (gRNA) was designed and selected in the E-CRISP (E-Crisp.org). The *TgAAT*-specific CRISPR knockout plasmids (pDF-Cas9-sgRH/PLKAAT, Fig. 7A) containing Cas9, GFP, guide RNA and dihydrofolate

reductase (*DHFR*) expression cassettes were generated by replacing the original targeting gRNA in pDF-PLK-GRA9 plasmid (Guo et al., 2019). RH and PLK of 10^7 tachyzoites were transfected with 10 μg of the pDF-Cas9-sgRH/PLKAAT plasmids, respectively, as previously described (Soldati and Boothroyd, 1993). The stable transformants based on pyrimethamine (1 μM) was selected as described previously (Donald and Roos, 1998; Reynolds et al., 2001). The stable knockout lines (*ΔRHaat* and *ΔPLKaat* strains) were isolated by limiting dilution in 96-well plates, and confirmed by PCR, Western blot and indirect fluorescent antibody test (IFAT).

Complement of *AAT* gene on *ΔRHaat* and *ΔPLKaat* strains

To complement the *AAT* gene in knockout strains, the full *TgAAT* fragment containing synonymous codons mutated at target sites of *AAT* for gRNA was amplified from RH and PLK cDNA by overlap PCR to generate the complemented *AAT* plasmids (pB-synoRHAAT and pB-synoPLKAAT, Fig. 7B) as described previously (Guo et al., 2019), respectively. The *ΔRHaat* and *ΔPLKaat* parasites (10^7 tachyzoites) were transfected with pHX-UPRT and linearized pB-synoRHAAT or pB-synoPLKAAT by *Sac* I (mass ratio, 1:5) (Roche, Switzerland) to generate complemented strains (ComRHAAT and ComPLKAAT strains) by insertion at the *UPRT* locus as described previously (Guo et al., 2019). Then the parasites were screened and selected with 10 μM 5-Fluorouracil compound (Sigma, USA). Stable complemented lines (ComRHAAT and ComPLKAAT strains) were isolated in 96-well plates with a limiting dilution, and confirmed by PCR, Western blot and IFAT. Positive clones were confirmed. All the plasmids obtained in th present study were verified and confirmed using DNA sequencing before use.

Plaque assay

To determine the effect on parasite growth after loss of *AAT* on RH and PLK strains, all strain parasites including wild-type, *Δaat* and ComAAT were used to perform the plaque formation, extracellular invasion, intracellular replication and egress assay *in vitro*, as well as virulence assay *in vivo* as described followed. All experiments were conducted in triplicate and repeated at least three times. The fresh purified tachyzoites (150 of RH and 300 of PLK per well) were inoculated onto monolayers of Vero cells or HFF in 12-well plate and grown for 8 days for RH and 12 days for PLK parasites at 37℃ in 5% CO_2. Subsequently, the samples were fixed by using 4% paraformaldehyde, stained with 0.1% crystal violet, and imaged on a scanner to analyze the plaque numbers and relative sizes, as described previously (Shen and Sibley, 2014).

Invasion assay

The invasion assay was performed by IFAT (Wang et al., 2017b). Vero cells (1×10^5 per well) were used to plate on 12-well cultured for 24 h. Fresh purified tachyzoites (2×10^5 per well) were inoculated onto cell monolayer for 2 h infection under normal growth conditions. The coverslips were washed with PBS 6 times to remove extracellular parasites and fixed. Then mouse anti-SAG1 polyclonal antibody diluted 1:500 and Alexa Fluor 594-conjugated goat anti-mouse IgG (Sigma, USA) diluted 1:1000 were used to count the number of attached parasites. After permeabilizing with 0.3% Triton X-100/PBS, rabbit anti-SAG1 polyclonal antibody diluted 1:500 and Alexa Fluor 488-conjugated goat anti-rabbit IgG with 1:500 dilution (Sigma, USA) were used to count the number of invading parasites as described previously (Guo et al., 2019). Samples were observed using the All-in-one Fluorescence Microscope (BZ-900, Keyence, Japan). The stained parasites with both red and green were noted as attached tachyzoites, while stained parasites with only in

green were noted as invaded tachyzoites. Ten fields were randomly counted for each sample of coverslip. All experiments of invasion assay were developed in triplicate and repeated at least three times.

Intracellular replication assay

The intracellular replication was determined by checking the number of tachyzoites each vacuole as previously described (Wang et al., 2017b). Vero cells (1×10^5 per well) were used to plate on 12-well cultured for 24 h. Fresh purified tachyzoites (2×10^5 per well) were inoculated onto cell monolayer for 2 h infection. Every well was washed with PBS 6 times to remove extracellular parasites and then cultured for 24 h or 32 h. Tachyzoites in vacuoles were stained with mouse anti-SAG1 antibody by the IFAT at 24 or 32 h post-infection and counted in at least 100 vacuoles. All experiments of replication were performed in triplicate and repeated at least three times.

Egress assay

Vero cells (1×10^5 per well) were used to plate on 12-well cultured for 24 h. Fresh purified tachyzoites (2×10^5 per well) were inoculated onto cell monolayers for 32 h infection under normal growth conditions as previously described (Guo et al., 2019). Firstly, the extracellular parasites will be removed by washing with PBS 5 times, and then 3 μM A23187 (Sigma, USA) was used to incubate cells. Followingly, fixed and IFAT was developed by using *T. gondii* specific antibodies including mouse anti-SAG1 and rabbit anti-GRA7. At least 300 vacuoles in this experiment were counted each well overslip to measure the rate of egressed PVs. All experiments of egress assay were conducted in triplicate and repeated at least three times.

Virulence tests in mice model

To determine the effect on parasite virulence after loss of *AAT* on RH and PLK strains, all six strain parasites including wild-type, *Δaat* and ComAAT were used to perform survival assay in mice. Fresh tachyzoites were purified and counted as described above, and then the different doses were used to inject into 7-week-old female BALB/c mice by intraperitoneal injection. Daily observations of mice were noted, such as body weight, morbidity, mortality and clinical signs. To record clinical symptoms, the clinical scores varied from 0 to 10, no signs, all sigs, respectively. In brief, the clinical symptoms included hunching, piloerection, worm-seeking, behavior, ptosis, sunken eyes, ataxia, the latency of movement, deficient evacuation and touch reflexes, and lying on belly (Leesombun et al., 2016; Guo et al., 2019). Surviving mice were monitored for 30 days and blood was drawn at day 30 to confirm infection using ELISA assay, as well as tissues were collected to determine parasite burdens through targeting of *TgB1* gene by quantitative PCR (qPCR). GraphPad Prism 7 (GraphPad Software, USA) was used to graph cumulative mortality as Kaplan–Meier survival plots and analyzed.

Metabolic treatment assay on *Δaat in vitro*

For metabolic treatment assay, α-ketoglutarate is dissolved in EMEM with 8% FBS, 100 U ml^{-1} penicillin and 100 mg ml^{-1} streptomycin to a final concentration of 400 μM or 2 mM. The parasites were cultured in Vero cells in EMEM containing α-ketoglutarate or normal EMEM to perform intracellular replication assay of 24 or 32 hour post-infection and plaque assay as described above, respectively. Subsequently, different phenotypes will be recorded and analyzed.

DNA isolation and quantitative PCR (qPCR) of parasite burdens in infected mice tissues

DNA was extracted from the tissue samples (brain, liver and spleen) of parasite challenged mice by DNeasy Blood & Tissue Kit (Qiagen, Germany), according to the manufacturer's instructions. The 200 ng tissues DNA was then amplified with specific primers targeting to the *T. gondii B1* gene (forward primer 5'- AAC GGG CGA GTA GCA CCT GAG GAG -3', the reverse primer 5'- TGG GTC TAC GTC GAT GGC ATG ACA AC -3') by qPCR. The standard curve was generated by using 10-fold serial dilutions of *T. gondii* DNA extracted from 10^5 parasites; thus, the curve ranged from 0.01 to 10,000 parasites. The parasite number was tested by using this standard curve. The amplification was performed with DNA, 1 × PowerUp™ SYBR™ Green Master Mix (Thermo Fisher Scientific, MA) and 500 nM gene-specific primers in 10 µl total reaction volume by a standard protocol recommended by the manufacturer (2 min at 50 ℃, 10 min at 95 ℃, then 40 cycles of 95 ℃ for 15 s and 60 ℃ for 1 min). Amplification, data acquisition, and data analysis were carried out in the ABI Prism 7900HT Sequence Detection System (Applied Biosystems, USA), and the cycle threshold values (C_t) were calculated as described previously (Mahmoud et al., 2015).

Total RNA extraction and qPCR analysis of gene expression

Total RNA was extracted from homogenized tissues (brain, liver and spleen) using TRI Reagent (Sigma, USA). The cDNA was amplified by Reverse transcription of 800ng RNA with PrimeScript™ RT Master Mix (Perfect Real Time) (TaKaRa Bio, Japan) according to the manufacturer's instructions. qPCR was carried out as described above. All primers were used in this study are listed in Table 3. The expression levels of target genes were normalized to Glyceraldehyde-3-phosphate dehydrogenase (*GAPDH*) mRNA levels using the $2^{\Delta\Delta Ct}$ method.

Cytokine ELISA

Previous studies reported that anti-*Toxoplasma* defense mechanisms depend largely on the interferon gamma (IFN-γ) production by immune cells (Yarovinsky and Sher, 2006). As well as, the tumor necrosis factor alpha (TNF-α) as a critical pro-inflammatory cytokine, is involved in the host's immune responses against parasites (Dégbé et al., 2018; Yang et al., 2018), and mediates apoptosis for T cells and NK cells predominantly (Mordue et al., 2001). Therefore, to explain currently enhanced acute virulence whether the *AAT*-deleted parasites in mice are associated with overstimulation of Th1 cytokines which led to lethal infections (Mordue et al., 2001), mouse serum was collected for measurement of IFN-γ and TNF-α levels using Mouse IFN gamma ELISA and TNF alpha mouse ELISA kit (Thermo Fisher Scientific, MA) according to the manufacturer's recommendations.

Statistical analysis

The GraphPad Prism 7 software (GraphPad Software Inc., USA) was used to graph and analyze the data. An unpaired Student's *t*-test, Tukey's Multiple Comparison Test, Chi-squre Test and one-way ANOVA plus Tukey-Kramer *post hoc* analysis were performed to do the statistical analyses in this study. Survival curves were analyzed using the Kaplan-Meier method and statistical comparisons developed with the log-rank method. Data represent the mean ± Standard Error of Mean. A p value < 0.05 was considered statistically significant (* $p < 0.05$, ** $p < 0.01$, *** $p < 0.001$ or **** $p < 0.0001$).

2-3. Results

Knockout *TgAAT* on RH and PLK strains

To investigate *AAT* in *T. gondii*, I proceeded to generate two knockout strains (*ΔRHaat* and *ΔPLKaat* strains) using pDF-Cas9-sgAAT plasmid (Fig. 7A), and two complemented strains (ComRHAAT and ComPLKAAT strains) using pB-synoRHAAT or pB-synoPLKAAT plasmids (Fig. 7B) containing codons synonymous to *TgAAT*s by the CRISPR/Cas9-mediated genome editing, respectively. Diagnostic polymerase chain reactions (PCRs) were developed to confirm single clones, and to check the gene deletions and complements. The *AAT* and *UPRT* genomic fragments were not amplified in knockout (Fig. 8A) and complemented (Fig. 8B) parasites while different fragments within plasmids were detected, respectively. After selection, *ΔRHaat* and *ΔPLKaat*, ComRHAAT and ComPLKAAT, and the wild-type strains were all verified by Western blot analysis (Fig. 8C). Protein bands were observed in the lysate of RH/PLK and ComRH/PLKAAT lines using specific anti-*Tg*AAT antibody, but not in the knockout strains. IFAT assay demonstrated that *TgAAT* was expressed in the wild-type and complemented parasites but not in the mutant strains (Fig. 8D). These data confirmed loss of *AAT* both in RH and PLK strains, and homologous integration and insertion of syno*AAT* in *UPRT* site in representative complement.

Disruption of *AAT* on RH and PLK strains slows parasite growth *in vitro*

To estimate the impact of *AAT* disruption on parasite growth *in vitro*, all strains were used to determine the production of plaques on Vero cells monolayers. Results showed that all strains were able to form plaques (Fig. 9A and C). Significantly smaller of plaque sizes were present in *ΔPLKaat* compared to PLK parasites whereas plaques of *ΔRHaat* and RH parasites showed no significant differences (Fig. 9B and D).

To better understand the phenotype related to the loss of *AAT*, the effects in the invasion, intracellular replication and egress was evaluated *in vitro*, which was compared to parental parasites growth under standard tachyzoite growth conditions. As shown in Fig. 9E, the deletion of *AAT* in RH strain significantly inhibited the parasite ability of invasion, replication and egress *in vitro*. Similar results were present in the loss of *AAT* in PLK (Fig. 9F). These results indicate that *AAT* is dispensable for the intracellular growth of parasites, but that the ability of parasites to spread *in vitro* is significantly impaired after deletion of *AAT* in both RH and PLK strains.

Treatment with α-ketoglutarate rescues the growth defect in *AAT*-deleted mutants

*Tg*AAT catalyzes glutamate into α-ketoglutarate, an important intermediate of carbon metabolism in mitochondria. To investigate whether the supplementation with α-ketoglutarate could rescue the defect of parasite growth in *AAT*-deleted parasites, rates of intracellular parasite replication under with or without α-ketoglutarate culture conditions were compared. The results showed that α-ketoglutarate supplementation (400 μM) significantly increased the 24 h replication rates in *AAT*-deficient parasites of RH strain (Fig. 10A) and PLK strain (Fig. 10B). A lack of more profound improvement by α-ketoglutarate may be due to poor uptake of this nutrient. Indeed, plaque formation was also examined, which resulted in the *AAT*-deleted PLK mutant forming significantly larger plaques in the presence of exogenous α-ketoglutarate (Fig. 10C and D). Interestingly, the high concentration of α-ketoglutarate (2 mM) led to faster intracellular replication of *AAT*-deficient parasites compared to parental PLK *in vitro* (Fig. 10E). Taken together, rescue of *AAT*-deleted mutants by α-ketoglutarate suggests that AAT plays an important role during *T. gondii* the nutrient uptake.

Loss of *AAT* in PLK strain does not abolish the virulence of parasites *in vivo*

To assess the degree of virulence of the *Δaat* mutants, mice were infected with increasing doses (10,000, 30,000, and 50,000 in PLK group parasites per mouse, and 100 in RH group parasites per mouse, respectively) of tachyzoites. At the infection dose of 100 tachyzoites per mouse, RH, *ΔRHaat* and ComRHAAT parasites caused all 100% mortality in 9 dpi with similar body weight (%) (Fig. 11A and B) and no differently acute symptoms (data not show). The infection dose of 1×10^4 PLK group tachyzoites did not lead mice to died, whereas at the dose of 3×10^4 and 5×10^4 *ΔPLKaat* caused 100% mortality with significant reduction of body weight (Fig. 11C and D). The virulence is even higher than wild-type PLK and ComPLKAAT.

Absence of *AAT* in PLK strain does not decrease parasite burdens in mice

To better clarify the virulence on *ΔPLKaat* parasites in mice, the dose of parasites was increased to 5×10^4 tachyzoites in the survival assay, and meanwhile determined the IFN-γ and TNF-α level in mouse sera at 2, 4, 6 and 8 days post-infection (dpi). All *ΔPLKaat* infected mice died at 7 and 8 dpi, while 83.3% mortality was obtained in PLK-infected mice however even at the highest infection dose of 5×10^4 tachyzoites per mouse (Fig. 11C and D). In addition, IFN-γ and TNF-α levels in sera from mice with *ΔPLKaat* infection were present in higher level at 2 and 4 dpi, and in significantly elevated levels at 6 and 8 dpi, compared to that of with PLK infection (Fig. 12A and B). Collectively, these current results indicated that loss of *AAT* in PLK caused a stronger as well as more serious immune response in mice during infection correlating with lethality.

The above results revealed that AAT inactivation causes enhanced virulence in mouse models. To elucidate the mechanisms underlying the changes, mouse models

were injected with 1×10^5 purified parasites challenge of either PLK, mutant or ComPLKAAT strains by i.p. to promote acute infection. At 3 and 6 dpi, tissue samples (brain, liver and spleen) were collected, and the number of parasites contained was detected using the quantitative PCR (qPCR) targeting *TgB1* gene using extracted DNA. As shown in Fig. 12C, the 200 ng tissues DNA were used to determine the number of parasites in brain, liver and spleen tissues during different tachyzoites infection, revealing that the number of PLK, *ΔPLKaat* and ComPLKAAT parasites found in all three tissues of infected mice with different loads on 3 and 6 dpi. Although the parasite number in liver increased to 580.2177 parasites at 6 dpi from 14.467 parasites at 3 dpi, parasite loads of *ΔPLKaat*-infected mouse liver (8960.715 parasites per 200 ng DNA) was 15.44 times than that of the PLK-infected mouse at 6 dpi. Nonetheless, the parasite load in *ΔPLKaat* mouse spleen (408.7724 parasites per 200 ng DNA) was similar to wild-type (414.663 parasites per 200 ng DNA) at 6 dpi. These data suggest that loss of *AAT* in PLK strains resulted in increasing parasite burdens in tissues during acute infection. Subsequently, high burdens led to up-regulated mRNA expression levels of interleukin-12p40 (*IL12p40*), *IFN-γ*, *TNF-α*, *IL10* and inducible nitric oxide synthase (*iNOS*) activities (Fig. 12D). In particular, the expression of *IFN-γ* in *ΔPLKaat* mice liver was 4.44-fold than that PLK mice at 6 dpi and 21.4-fold than that of *ΔPLKaat*-infected mice at 3 dpi. Moreover the *iNOS* of *ΔPLKaat* mouse liver was up-regulated by 9.44-fold compared to that of PLK mouse liver at 6 dpi. Taken together, mice were infected with *AAT*-deficient parasites resulted to increased parasite numbers leading to up-regulate expression of inflammatory cytokines or *iNOS* in tissues as infection progressed, which induced overexpression of IFN-γ and TNF-α until a lethal outcome.

2-4. Discussion

With the advent of the genomic era, the widespread application of the CRISPR/Cas9 system has permitted precise and efficient genetic manipulations in *T. gondii* (Shen et al., 2017), such as gene editing and gene deletion, the purpose and significance are to identify specific genes with the important functions in the growth development of *T. gondii* or involved in the virulence or metabolic pathways, as well as to design and find important specific targets for drug action and safe vaccine antigen candidates. Therefore, the CRISPR/Cas9 system was used in current study to functionally analyze *T. gondii AAT* gene on type I RH and type II PLK strains.

In this study, two knockout strains and two complemented strains were successfully generated focusing on *TgAAT*. It is known that the asexual growth of *T. gondii* involves complete rounds of lytic cycles, which comprise invasion, replication, egress, and reinvasion of neighboring host cells (Nitzsche et al., 2016). Current results revealed that loss of *AAT* both in RH and PLK strains changed the development of complete rounds of lytic cycles observed in decreasing growth of parasites *in vitro*. Furthermore, the previous sequence alignment of predicted amino acid showed that several different amino acids present in the sequence of *AAT* between RH and PLK strains, whereas the expression level was similar in two parasite strains, indicating that *AAT* is encoded in both strains with similar role. As expected, the results showed similar growth phenotypes were determined in *AAT*-deficient parasites between in RH and PLK *in vitro*, suggesting a similar role of AATs for parasite growth present in native parasites of two type strains.

On the other hand, above results showed that the *T. gondii* AAT protein catalyzes the reversible of conversion of oxaloacetate and glutamate to aspartate and α-ketoglutarate as in *Plasmodium*. In *T. gondii*, AAT might mainly involve in

transforming glutamate into α-ketoglutarate, an important intermediate of carbon metabolism in mitochondria. To investigate whether α-ketoglutarate supplementation can rescue the growth defect in *AAT*-deleted parasites, levels of intracellular replication under culture conditions with the different doses of α-ketoglutarate were compared. Interestingly, the growth defect due to loss of *AAT* was significantly rescued by treatment with α-ketoglutarate (400 μM). Furthermore, the high concentration (2 mM) of α-ketoglutarate led to faster intracellular replication of *AAT*-deficient parasites compared to parental PLK *in vitro*. This denotes that loss of *AAT* in *T. gondii* impairs α-ketoglutarate homeostasis which is related to parasite growth *in vitro*. This finding may also explain why deficiency of *AAT* in PLK caused parasites to proliferate faster in mice (Fig. 12), considering that mice have higher metabolic α-ketoglutarate. High parasite burdens led to unexpected upregulation of cytokines and a lethal outcome, attributed to the enhanced virulence of PLK *in vivo*, in accordance with previous investigations (Suzuki et al., 1988; Mordue et al., 2001). All findings indicate that although *AAT* is not essential to the parasite growth under standard culture conditions, it plays a central role in the complex metabolic balance of α-ketoglutarate metabolism, which is largely involved in the carbon skeletons via glutamine metabolism as in *P. falciparum* (Berger et al., 2001; Jain et al., 2010; Wrenger et al., 2011; MacRae et al., 2012; Jacot et al., 2016).

However, the virulence assay demonstrated that the disruption of *AAT* on RH and PLK strain did not abolish parasite virulence *in vivo*. Regrettably, the results showed the different phenotypes of PLK *AAT*-deleted mutants between *in vivo* and *in vitro* is that although loss of *AAT* in PLK parasite significantly reduced parasite growth, the *AAT*-deficient mutant parasites did not abolish the acute virulence in BALB/c mice was observed. This confirmed the fact that the deleted *AAT* parasite growth under

different culture conditions between *in vitro* and *in vivo* will show the different phenotypes. It is also questionable whether two inhibitors (hydroxylamine and carboxymethoxylamine) could specifically target AAT, although above studies also observed that the inhibitors can inhibit specifically r*Tg*AAT enzymatic activity *in vitro*. To explain the difference, considering that the *AAT*-deficient parasites in type II strains present faster replication than wild-type parasite in infected mice, and this led mouse to induce excessive inflammatory reaction probably causes lethal toxoplasmosis. However, current studies could not explain why the absence of *AAT* caused much higher parasite burdens in mice, but it may assume that *AAT*-deficient may lead PLK parasites preferring to enter the more metabolically nutrient environment for proliferation, such as liver, which is consistent with the high concentration of α-ketoglutarate causes faster intracellular replication of *AAT*-deficient parasites than parental PLK *in vitro*.

2-5. Summary

In summary, the pathway of the conversion intermediate glutamate to α-ketoglutarate in glutaminolysis was focused in this study. *T. gondii* genome contains one the aspartate aminotransferase (AAT) enzyme to involve in speculation on a possible architecture of the pathway. Here, the functional analysis of the predicted AAT enzymes of these in both *T. gondii* type I RH and type II PLK strains was performed using the CRISPR/Cas9 gene-editing system. Current study indicates that although *AAT* is not essential to the parasite growth under optimal culture conditions, it plays an important role at least in α-ketoglutarate metabolism of glutamine pathway. Furthermore, although the present results confirm that deficiency of *AAT* both in RH and PLK inhibited the parasite ability of invasion, replication, egress and plaque

formation *in vitro*, the PLK *AAT*-deleted mutant parasites did not decrease the acute virulence in mice, which might be explained by the parasites grow under different cultural conditions between *in vitro* and *in vivo* leading to the different phenotypes of the *AAT*-deleted mutant parasites.

Table 2. Primers used for generation of *ΔRH/PLKaat* and ComRH/PLKAAT strains.

Primer name	Sequence(5'→ 3')	Use
RH/PLKAATgRNA-KOF1	CG*AAT*TGGAGCTCCACCGCGGGAGCTCCAAGTAAGCAGAAG	Construction of pDF-Cas9-sgRH/PLK*AAT*
RH/PLKAATgRNA-KOR1	AGGTTCACTTTTCTTGGGTCAACTTGACATCCCCATTTAC	Construction of pDF-Cas9-sgRH/PLK*AAT*
RH/PLKAATgRNA-KOF2	GACCCAAGAAAAGTGAACCTGTTTTAGAGCTAGA*AAT*AGC	Construction of pDF-Cas9-sgRH/PLK*AAT*
RH/PLKAATgRNA-KOR2	TCTAGAGCGGCCGCCACCGCGGGAGCTGATACCGCTCGCC	Construction of pDF-Cas9-sgRH/PLK*AAT*
RH/PLKsynoAAT-COF1	CTTTGAAGA*AAT*CAAGCAAGG*AAT*TCATGTTTCCAACTCTTAGTGA	Construction of pB-synoRH/PLK*AAT*
RH/PLKsynoAAT-COR1	AGATTGACTTTTCTTGGGTCTTGGTCTGCCCTGAACGCGA	Construction of pB-synoRH/PLK*AAT*
RH/PLKsynoAAT-COF2	GACCCAAGAAAAGTC*AAT*CTCGGCATCGGAGCCTACCGAA	Construction of pB-synoRH/PLK*AAT*
RH/PLKsynoAAT-COR2	TTAAGCGT*AAT*CTGGAACATCGTATGGGTACATGCTTGCAGGAACTGCCCGCA	Construction of pB-synoRH/PLK*AAT*
ΔRH/PLKaat-CheckP1	GCACTCAACAGAGGGTATTT	Validation of *Δaat*, PCR1
ΔRH/PLKaat-CheckP2	CACCCGAGCTGGCTTGCTTA	Validation of *Δaat*, PCR1
ΔRH/PLKaat-CheckP3	CG*AAT*TGGAGCTCCACCGCGGGAGCTCCAAGTAAGCAGAAG	Validation of *Δaat*, PCR2
ΔRH/PLKaat-CheckP4	TCTAGAGCGGCCGCCACCGCGGGAGCTGATACCGCTCGCC	Validation of *Δaat*, PCR2
ComRH/PLKAAT-CheckP5	TCTTCTACGCCGACCGCCTGATT	Validation of ComRH/PLKAAT, PCR3
ComRH/PLKAAT-CheckP6	CAGGCAGCTTCTCGTAGATCAG	Validation of ComRH/PLKAAT, PCR3
ComRH/PLKAAT-CheckP7	TTCAGACTCTCTGTGGTCGGCGAG	Validation of ComRH/PLKAAT, PCR4
ComRH/PLKAAT-CheckP8	ATGGTCAACAAAACAGCATATTCCTCCC	Validation of ComRH/PLKAAT, PCR4
ComRH/PLKAAT-CheckP9	GTAGAGAGGACCAAAAGACGATTGC	Validation of ComRH/PLKAAT, PCR5
ComRH/PLKAAT-CheckP10	CGAACCGATATA*AAT*GCATGGCAT	Validation of ComRH/PLKAAT, PCR5

Table 3. Primers used quantitative PCR (qPCR).

Target gene		Forward Primer (5'→ 3')	Reverse Primer (5'→ 3')
T. gondii	*B1*	AACGGGCGAGTAGCACCTGAGGAG	TGGGTCTACGTCGATGGCATGACAAC
Mouse	*IL-12p40*	GAGCACTCCCCATTCCTACT	ACGCACCTTTCTGGTTACAC
	IFN-γ	GCCATCAGCAACAACATAAGCGTC	CCACTCGGATGAGCTCATTG*AAT*G
	TNF-α	GGCAGGTCTACTTTGGAGTCATTGC	ACATTCGAGGCTCCAGTGAA
	IL10	TGGACAACATACTGCTAACCGAC	CCTGGGGCATCACTTCTACC
	iNOS	ACCCCTGTGTTCCACCAGGAGATGTTGAA	TGAAGCCATGACCTTTCGCATTAGCATGG
	GAPDH	TGTGTCCGTCGTGGATCTGA	CCTGCTTCACCACCTTCTTGAT

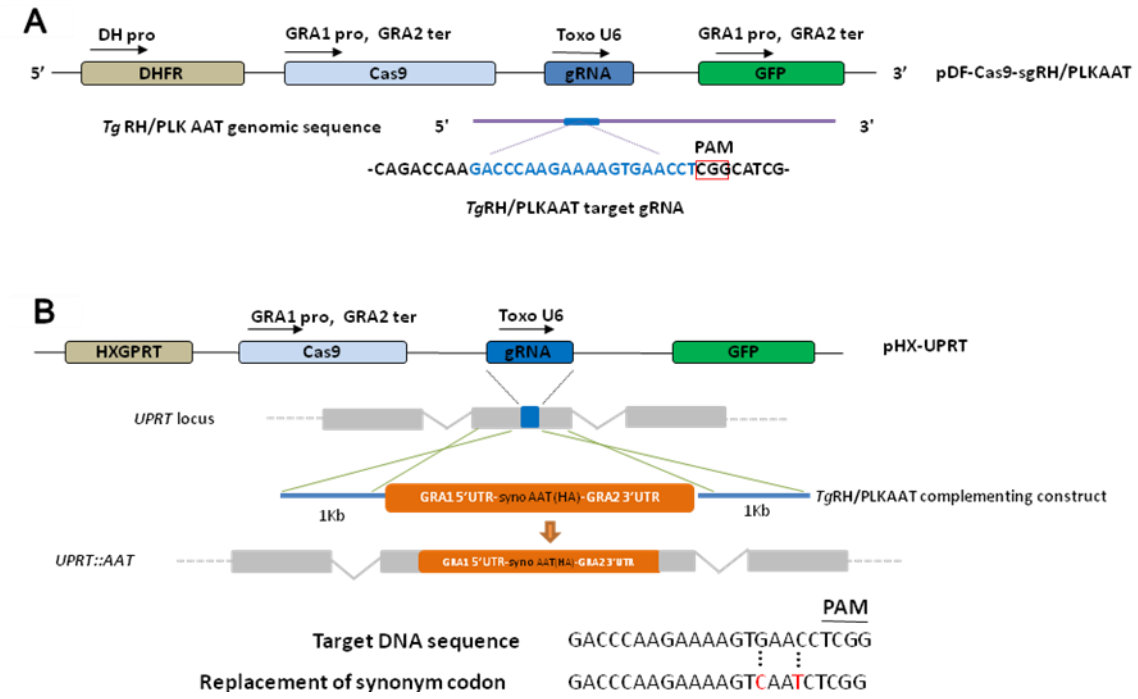

Fig. 7. Knockout *TgAAT* on RH and PLK strains. (A) Schematic illustration of knocking out *AAT* by CRISPR/Cas9 system both in RH and PLK strains, including Cas9, GFP, guide RNA and dihydrofolate reductase (*DHFR*) expression cassettes expressed in different colors. (B) Schematic of CRISPR/Cas9 strategy for insertion of syno*AAT* in *UPRT* locus. The blue bar in *UPRT* gene represents the region targeted by the gRNA.

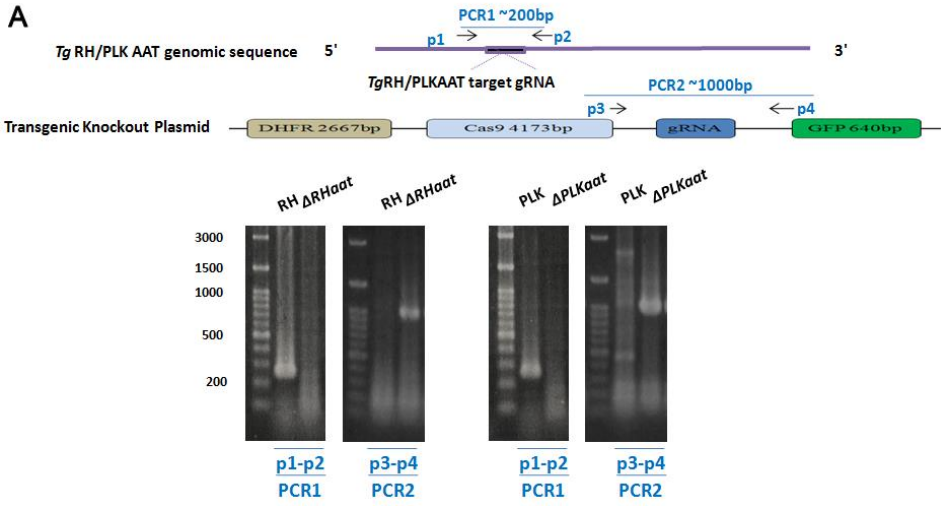
A
PCR1 ~200bp
p1
p2
Tg RH/PLK AAT genomic sequence
5'
3'
TgRH/PLKAAT target gRNA
PCR2 ~1000bp
p3
p4
Transgenic Knockout Plasmid
DHFR 2667bp
Cas9 4173bp
gRNA
GFP 640bp
RH ΔRHaat
RH ΔRHaat
PLK ΔPLKaat
PLK ΔPLKaat
3000
1500
1000
500
200
p1-p2
PCR1
p3-p4
PCR2
p1-p2
PCR1
p3-p4
PCR2

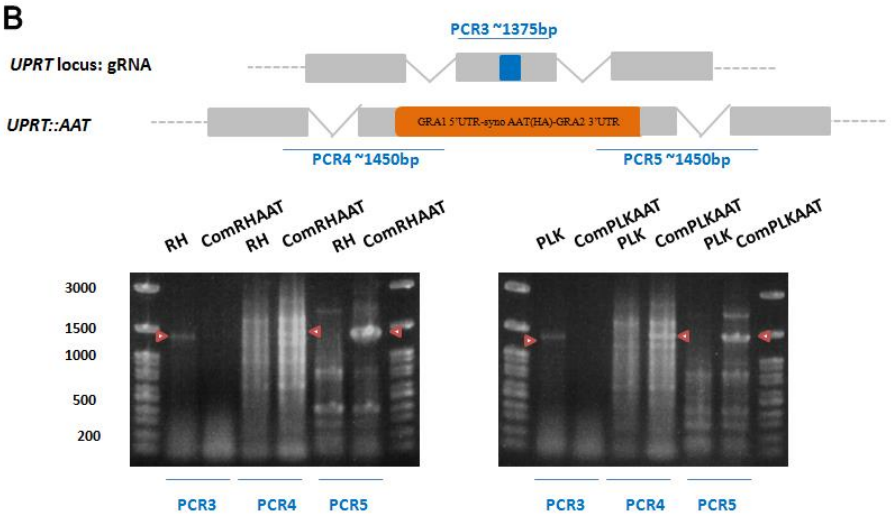
B
PCR3 ~1375bp
UPRT locus: gRNA
UPRT::AAT
GRA1 5'UTR-syno AAT(HA)-GRA2 3'UTR
PCR4 ~1450bp
PCR5 ~1450bp
RH ComRHAAT
RH ComRHAAT
RH ComRHAAT
PLK ComPLKAAT
PLK ComPLKAAT
PLK ComPLKAAT
3000
1500
1000
500
200
PCR3
PCR4
PCR5
PCR3
PCR4
PCR5

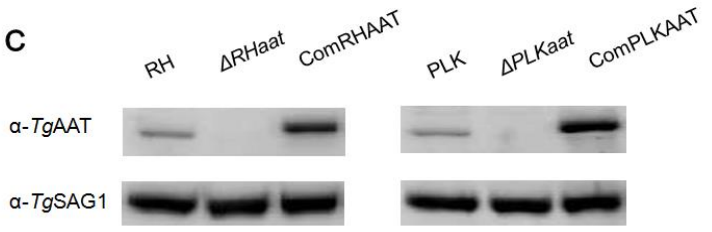
C
RH
ΔRHaat
ComRHAAT
PLK
ΔPLKaat
ComPLKAAT
α-TgAAT
α-TgSAG1

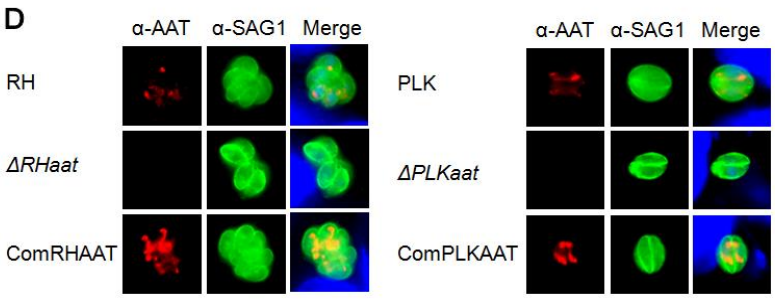
D
α-AAT
α-SAG1
Merge
α-AAT
α-SAG1
Merge
RH
ΔRHaat
ComRHAAT
PLK
ΔPLKaat
ComPLKAAT

Fig. 8. Confirmation of strains among *ΔRHaat*, *ΔPLKaat*, ComRHAAT and ComPLKAAT compared with wild-type RH and PLK strains. (A and B) Confirmation of knockout by PCR. PCR1/PCR2 denotes the amplification products of diagnostic polymerase chain reactions (PCRs) from *ΔRHaat* and *ΔPLKaat* parasites. PCR3/PCR4/PCR5 denotes the amplification products of PCRs from ComRHAAT and ComPLKAAT parasites. (C) Western blot analysis of *Δaat* and ComAAT parasites. Wild-type strains RH and PLK were used as control. (D) IFAT analysis of *Δaat* and ComAAT parasites. Wild-type strains RH or PLK were used as control. Mouse α-*Tg*RH/PLKAAT and rabbit α-*Tg*SAG1 antibody was used for staining.

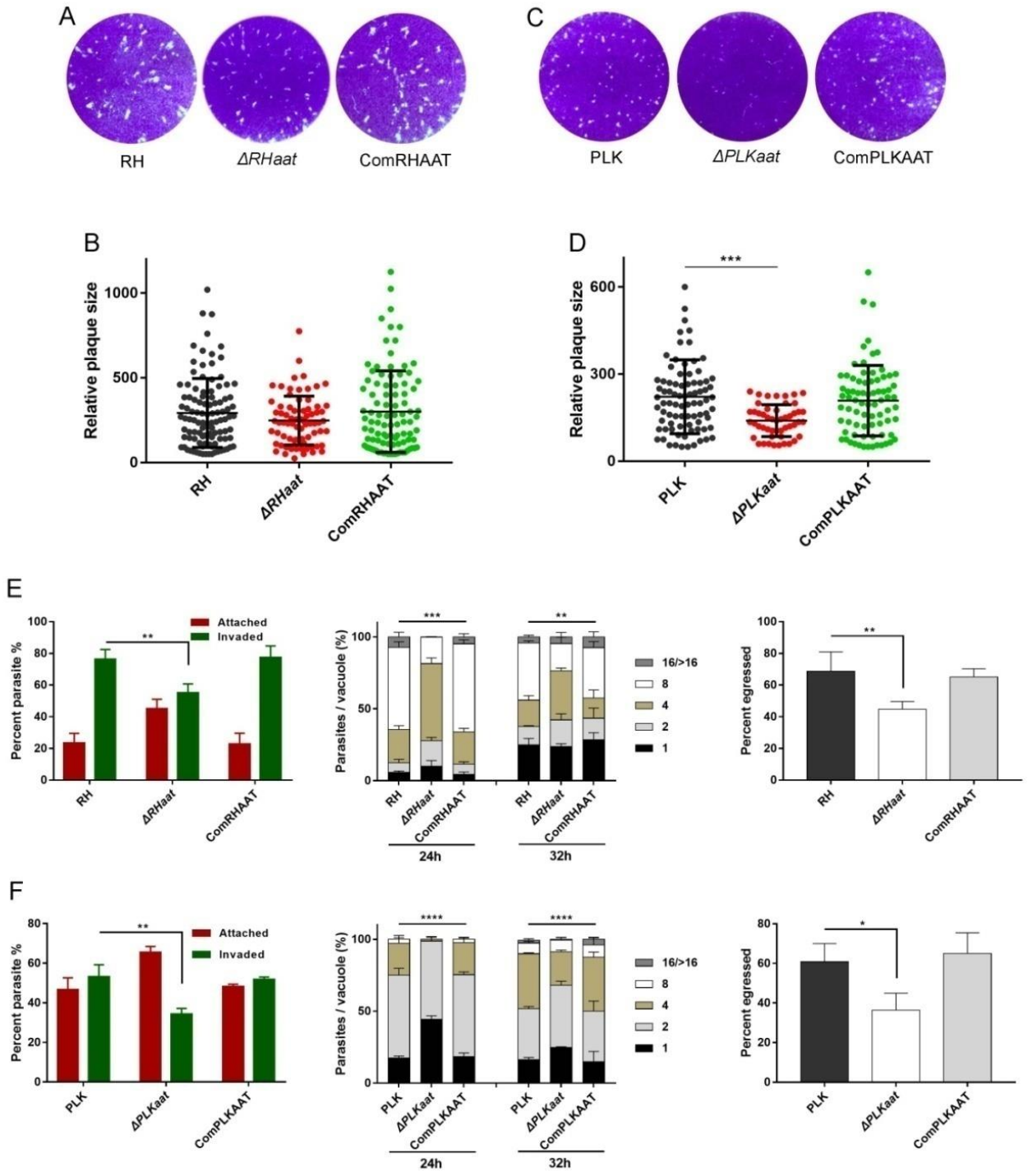

Fig. 9. *AAT*-deficiency slows down RH and PLK parasite growth *in vitro*. (A) Plaque assay. The growth of 150 *Δaat* or ComAAT tachyzoites *in vitro* was compared with the parental RH strains. Plaque was visualized by staining with 0.1% crystal violet. (B)

Relative size of plaques in A. The data are presented as the mean ± SEM of three independent experiments. (C) Plaque formation of *ΔPLKaat in vitro*. Vero cells were infected by 300 tachyzoites, cultured for 12 days. (D) Relative size of plaques in panel C. The data are presented as the mean ± SEM of three independent experiments. *** $p < 0.001$, one-way ANOVA plus Tukey-Kramer *post hoc* analysis. (E and F) Invasion, replication and egress assay of mutants compared to parental and complemented strains in RH (E) and PLK (F) lines. The data are presented as the mean ± SEM of at least three independent experiments. * $p < 0.05$, ** $p < 0.01$, *** $p < 0.001$, **** $p < 0.0001$, determined by Chi-square Test (invasion and egress assay) and Tukey's Multiple Comparison Test (replication assay).

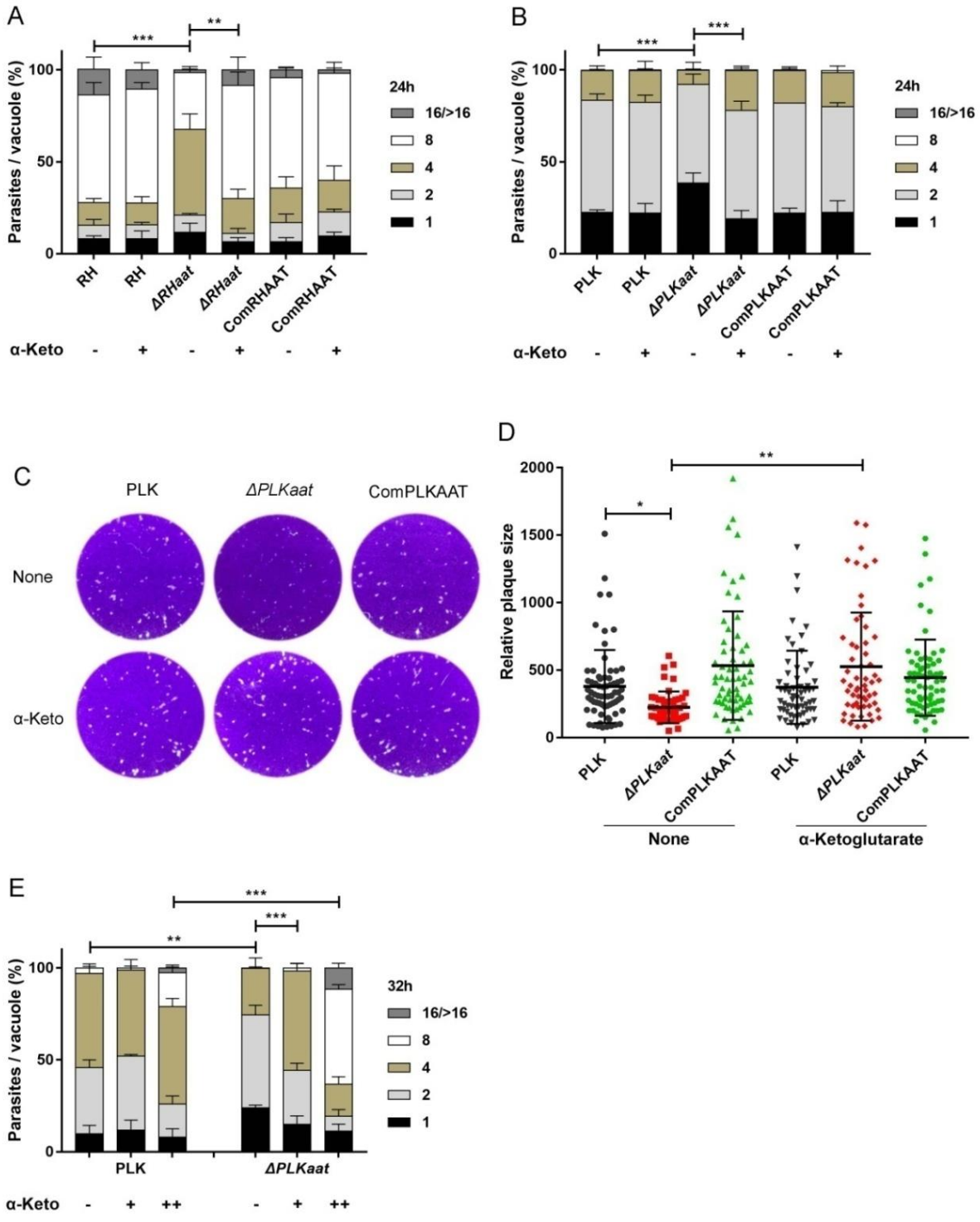

Fig. 10. Supplementation with α-ketoglutarate (α-Keto) rescues growth defects in *Δaat*. (A) Supplementation assay with α-ketoglutarate (400 μM) on type 1 strain RH.

The tachyzoites growth with or without α-ketoglutarate 24 hour post-infection, and the number of parasites in each PV were then determined. (B) PLK replication rescues by α-ketoglutarate (400 μM). Infected tachyzoites were cultured in Vero cells with or without α-ketoglutarate for 24 h, and then the number of parasites in each PV was determined. (C) Plaque formation of *ΔPLKaat* under α-ketoglutarate supplementation conditions. (D) Relative size of plaques in panel C. (E) The high concentration of α-ketoglutarate (2 mM) led to faster replication of *AAT*-deficient parasites compared to parental PLK *in vitro*. The data are presented as the mean ± SEM of three independent experiments. – no treatment with α-ketoglutarate, + treatment by low concentration of 400 μM, ++ treatment by high concentration of 2 mM. * $p < 0.05$, ** $p < 0.01$, *** $p < 0.001$, one-way ANOVA plus Dunnett's multiple comparisons test (replication assay) and one-way ANOVA plus Tukey-Kramer *post hoc* analysis (plaque assay).

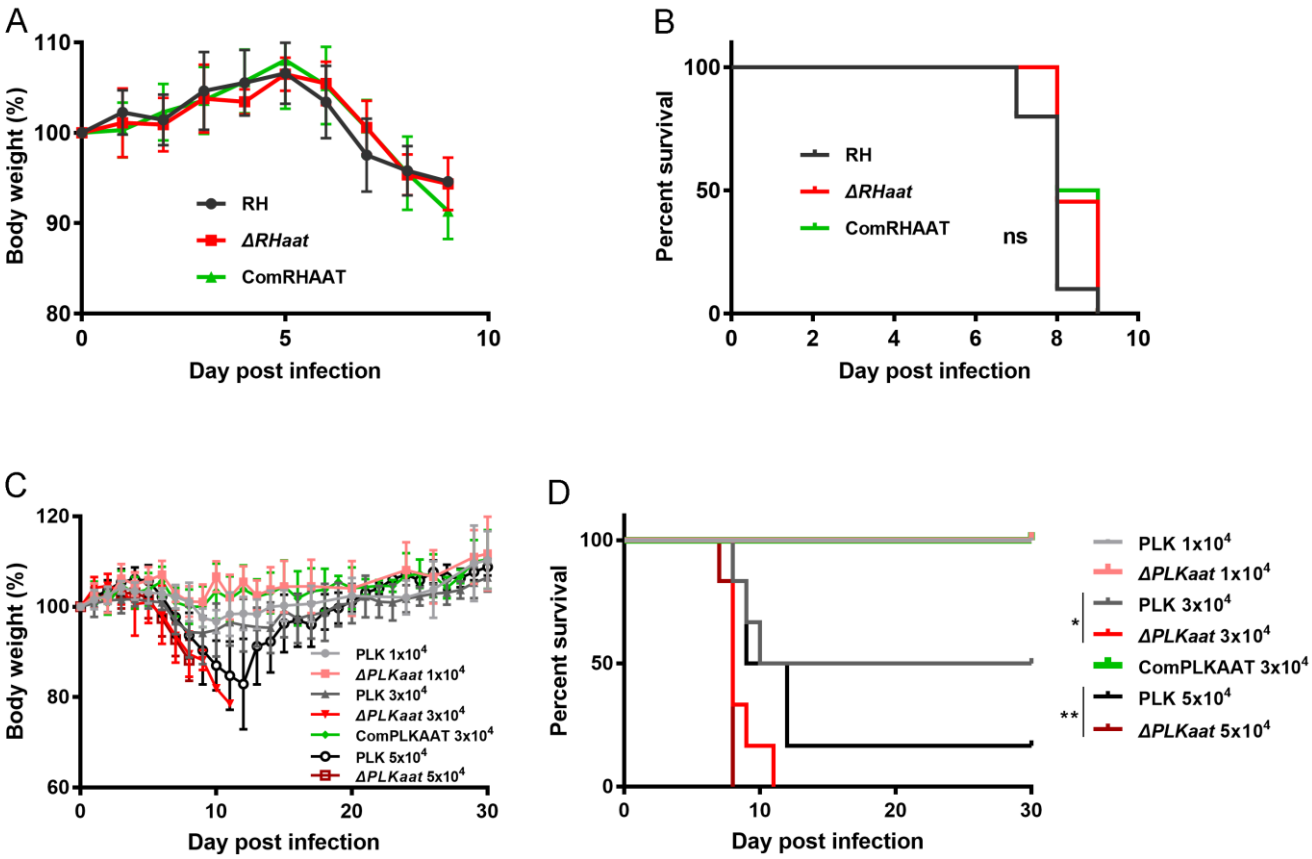

Fig. 11. Virulence tests of *Δaat* in mice. (A and B) Body weight % (A) and survival rate (B) during *ΔRHaat* infection. Mice were infected by intraperitoneal injection with 100 tachyzoites of RH (n = 11), *ΔRHaat* (n = 11) and ComRHAAT (n = 6). (C) Body weight during *ΔPLKaat* infection. Six mice were infected with 10,000, 30,000 and 50,000 tachyzoites by intraperitoneal injection. (D) The survival rate of PLK *AAT*-deficiency parasite infection in mice. Survival curves of mice infected with *ΔPLKaat* tachyzoites was noted until day 30. * $p < 0.05$, ** $p < 0.01$, Log-rank (Mantel-Cox) test.

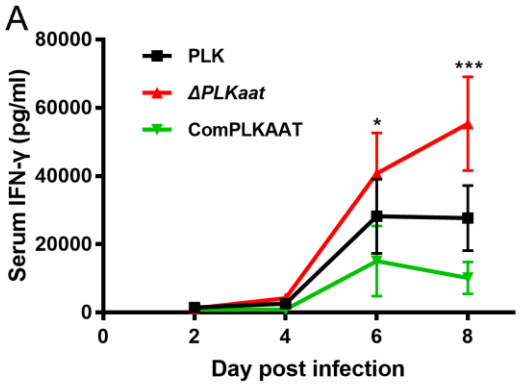
A
Serum IFN-γ (pg/ml)
80000
60000
40000
20000
0
PLK
ΔPLKaat
ComPLKAAT
*
***
0
2
4
6
8
Day post infection

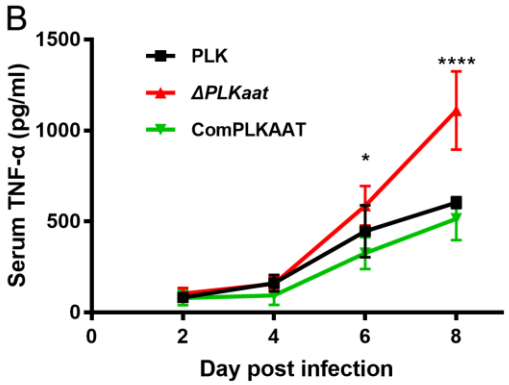
B
Serum TNF-α (pg/ml)
1500
1000
500
0
PLK
ΔPLKaat
ComPLKAAT
*
****
0
2
4
6
8
Day post infection

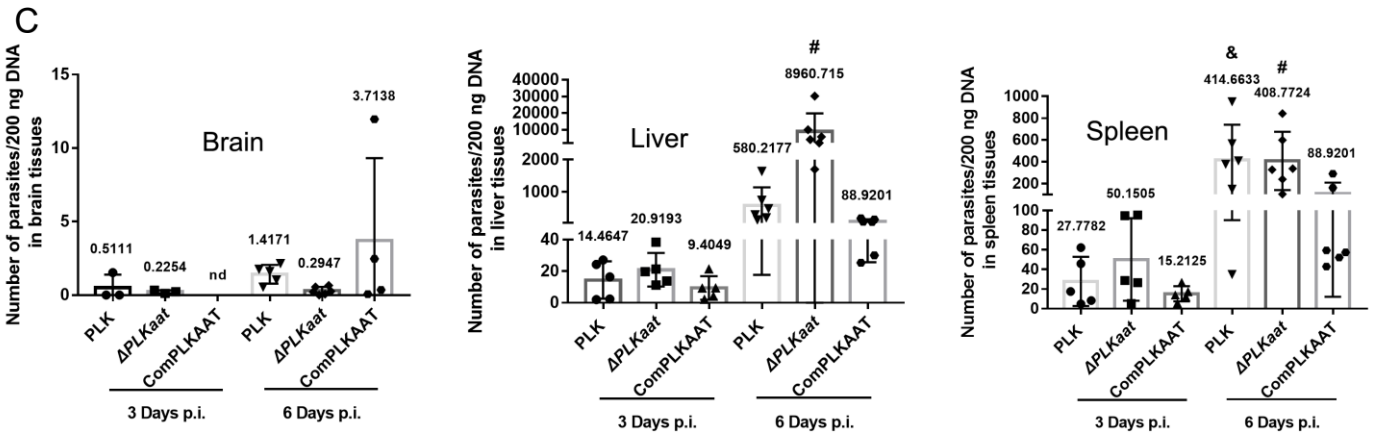
C
Number of parasites/200 ng DNA in brain tissues
Brain
0.5111
0.2254
nd
1.4171
0.2947
3.7138
Number of parasites/200 ng DNA in liver tissues
Liver
14.4647
20.9193
9.4049
580.2177
8960.715
88.9201
#
Number of parasites/200 ng DNA in spleen tissues
Spleen
27.7782
50.1505
15.2125
414.6633
408.7724
88.9201
&
#
PLK
ΔPLKaat
ComPLKAAT
3 Days p.i.
6 Days p.i.

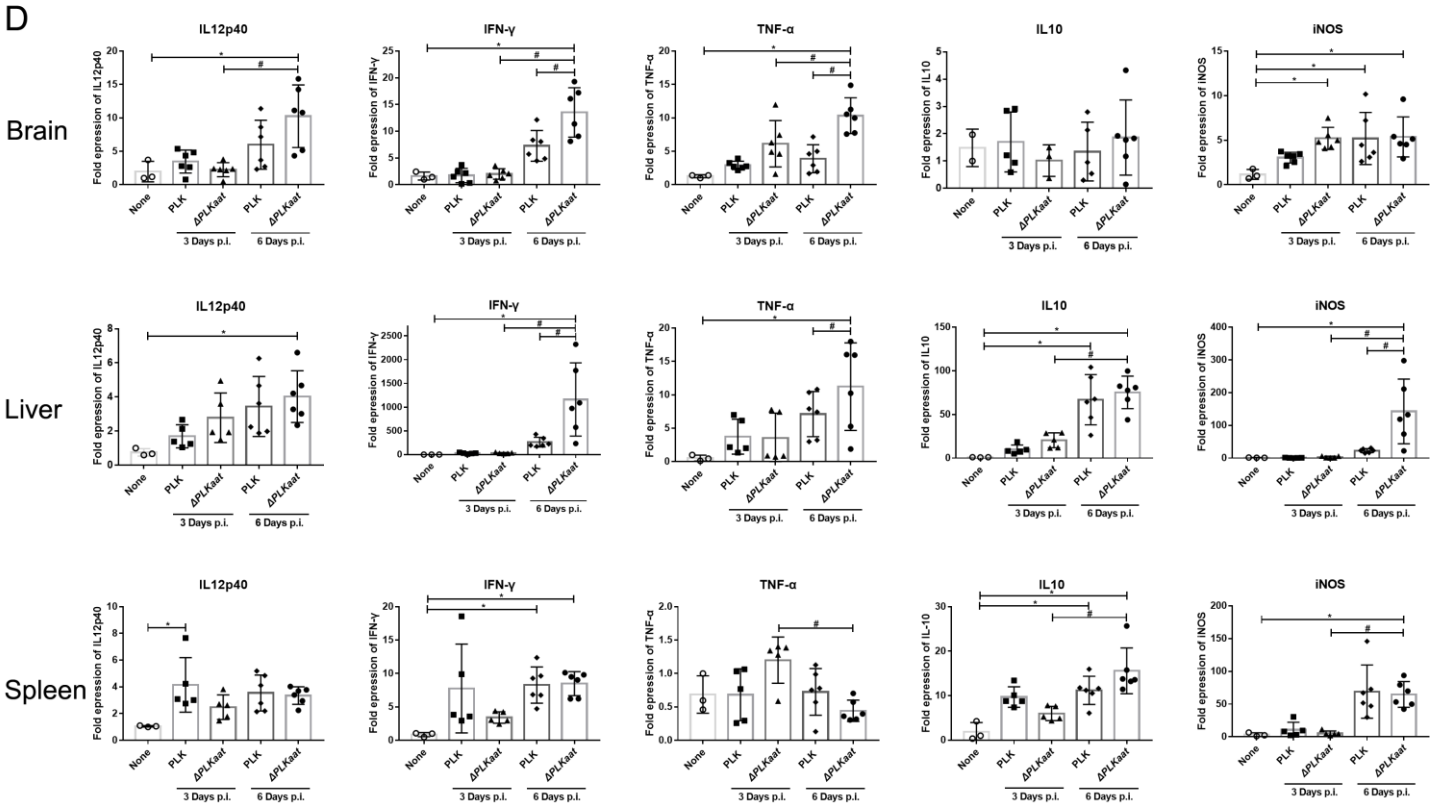
D
Brain
Liver
Spleen
IL12p40
IFN-γ
TNF-α
IL10
iNOS
Fold epression of IL12p40
Fold epression of IFN-γ
Fold epression of TNF-α
Fold epression of IL10
Fold epression of IL-10
Fold epression of iNOS
None
PLK
ΔPLKaat
3 Days p.i.
6 Days p.i.

Fig. 12. *ΔPLKaat* infection causes higher parasite burdens in mice. (A and B) Serum IFN-γ (A) and TNF-α (B) level of 50,000 *ΔPLKaat* tachyzoites challenge by intraperitoneal injection. Mouse sera were collected at 2, 4, 6 and 8 dpi by Tail tip. IFN-γ and TNF-α was detected by ELISA. * $p < 0.05$, ** $p < 0.01$, *** $p < 0.001$, one-way ANOVA plus Tukey-Kramer *post hoc* analysis. (C) Parasite burdens during acute infection. Six mice were infected by intraperitoneal injection with 100,000 tachyzoites, and then tissues including brain, liver and spleen were collected at 3 or 6 dpi. Parasite burdens were determined from tissues DNA by qPCR. # $p < 0.05$ vs. day 6 *ΔPLKaat* group; & $p < 0.05$ vs. day 6 PLK group, one-way ANOVA plus Tukey-Kramer *post hoc* analysis. (D) The expression of inflammatory cytokines and *iNOS* during acute *ΔPLKaat* infection in mice. * $p < 0.05$ vs. no-infection group; # $p < 0.05$ vs. day 6 *ΔPLKaat* group, one-way ANOVA plus Tukey-Kramer *post hoc* analysis.

Chapter 3

Hydroxylamine and carboxymethoxylamine inhibit *Toxoplasma gondii* growth through an aspartate aminotransferase-independent pathway

3-1. Introduction

Previous studies demonstrated that AAT of *Plasmodium falciparum* catalyzes the reversible reaction of aspartate and α-ketoglutarate to glutamate (Wrenger et al., 2011; Wrenger et al., 2012; Jacot et al., 2016), which are important intermediates to develop carbon metabolism and amino acid cycle for parasite surviving. Hydroxylamine (HYD) and carboxymethoxylamine (CAR), are inhibitors of AATs, abolish almost the transamination activity of r*Pf*AAT and interfere with the proliferation of the parasite (Marković-Housley et al., 1996; Berger et al., 2001; Wrenger et al., 2011; Wrenger et al., 2012). The *PfAAT* was believed to be good drug targets. However, effects of HYD and CAR, and their relationship with AAT on *Toxoplasma gondii* remain unclear.

Although the above studies reveal that the deleted *AAT* parasites obtained showed different phenotypes under different culture conditions between *in vitro* and *in vivo*, the inhibition of reaction of r*Tg*AAT by HYD and CAR treatment was found. Hence, the anti-*T. gondii* potential of HYD and CAR *in vitro* and *in vivo* was evaluated in this chapter. The data indicated that HYD and CAR have the potential for treating toxoplasmosis even acute *T. gondii* infection through an AAT-independent pathway.

3-2. Materials and methods

Animals

Female BALB/c mice with a six-week-old were purchased from the Clea Japan for survival assay. Mice were maintained in the animal facility in the National Research Center for Protozoan Diseases, Obihiro University of Agriculture and Veterinary Medicine, as described above. All animal and pathogen experiments have strictly followed the Committee on the Ethics of Animal Experiments or Pathogen Experiments of Obihiro University of Agriculture and Veterinary Medicine, Japan, as described above.

Parasites culture

T. gondii type I RH-GFP strain (a RH strain with green fluorescent protein expressing) (Nishikawa et al., 2003), type I RH strain with hypoxanthine-xanthine-guanine phosphoribosyl transferase (*HXGPRT*) deficiency, PLK strain (type II), *ΔRHaat*, ComRHAAT, *ΔPLKaat*, and ComPLKAAT were used in the present study. All parasites were cultured in Vero or HFF cells, and purified using 27-gauge needle syringe and 5.0-μm pore filter, as described above.

Chemicals

Hydroxylamine (HYD) and carboxymethoxylamine hemihydrochloride (CAR) were purchased from Sigma (catalog no. 7803-49-8 and 86-08-8). The inhibitors were dissolved in double distilled water (DDW) and dimethyl sulfoxide (DMSO), respectively, and stored at -30 ℃ until use.

Cytotoxicity analysis of HYD and CAR on HFF and Vero cells

Cytotoxicity of the two compounds were determined both on HFF and Vero cells using Cell Counting Kit-8 (CCK-8, Dojindo Molecular Technologies, Japan)

according to the manufacturer's instructions. Briefly, cells were plated in 96-well plates at a density of 1×10^4 cells per well of HFF or 1×10^5 of Vero, then incubated for 48 h (HFF cells) or 24 h (Vero cells) at 37 ℃ in a 5% CO_2 atmosphere. Then cells were exposed to the compounds with the final concentrations of 1, 5, 10, 25, 50, 100, 200, 400, 800 and 1000 μg/ml for 24 h, added with CCK-8 reagent react for 4 h. The absorbance of the supernatant was measured at 450 nm by an MTP-120 micro plate reader (Corona Electric, Japan). Cell viability (%) was calculated in three independent experiments together.

Inhibition assay of HYD and CAR on *T. gondii in vitro*

To evaluate anti-*T. gondii* potential *in vitro*, growth inhibition assay was performed with the two inhibitors and sulfadiazine (Sigma-Aldrich, USA). Purified 5×10^4/well RH-GFP tachyzoites were used and added into 96-well plates where HFF cells were seeded (1×10^4 cells/well) and cultured for 48 h. After 4 h, extracellular parasites were washed out. Then, the compounds at final concentrations of 1, 3.125, 6.25, 12.5, 25 and 50 μg/ml in HYD cultures or 1, 5, 10, 15, 20, 25, 50 and 100 μg/ml in CAR cultures were added, respectively. Medium and sulfadiazine (1 mg/ml) were used as negative and positive controls, respectively. The fluorescence intensity of RH-GFP parasites was measured using a microplate reader (SH-900, Corona Electric Co., Ltd, Ibaraki, Japan) after 72 h of incubation. Each concentration was determined in three independent experiments, together to calculate the half maximal inhibitory concentration (IC_{50}) values on *T. gondii* by GraphPad Prism 7 software (GraphPad Software Inc., CA).

Plaque assay

To examine the effects of compounds on parasite growth, in this study, the final concentration of 2-fold or 4-fold IC_{50} compounds, DMSO and sulfadiazine (1 mg/ml) were used to perform plaque formation, extracellular invasion, intracellular replication and egress assay on RH parasites as follows. The fresh purified tachyzoites (150 of RH) were inoculated onto monolayers of Vero cells or HFF in 12-well plate, and for compounds assay, after 2 h post parasites infection, old medium was replaced by the new medium with 2-fold or 4-fold IC_{50} values of compounds and DMSO, and were cultured for 8 days at 37℃ in 5% CO_2. Subsequently, samples were fixed by 4% paraformaldehyde, stained with 0.1% crystal violet, and imaged on a scanner to analyze the number and relative size of plaques, as described above. All assays were conducted in triplicate and repeated at least three times.

Invasion assay

Vero cells (1×10^5 per well) were used to plate on 12-well cultured for 24 h. For compounds assay, tachyzoites (2×10^5) were pretreated with either of the two compounds of 2-fold or 4-fold IC_{50} values, sulfadiazine (1 mg/ml), or DMSO for 1 h at 37 ℃, and then cultured for 2 h. The stained parasites with both red and green were noted as attached tachyzoites, while stained parasites with only in green were noted as invaded tachyzoites. Ten fields of per coverslip were randomly counted. All assays were preformed in triplicate and repeated at least three times.

Intracellular replication assay

Vero cells (1×10^5 per well) were used to plate on 12-well cultured for 24 h. Fresh purified tachyzoites (2×10^5 per well) were inoculated onto cell monolayer for 2 h infection under normal growth conditions. In the assay of examination of compounds effects for replication, after 2 h post-infection under standard growth conditions, the

new medium with 2-fold or 4-fold IC_{50} of compounds was added into cell well, cultured for 24 h. The number of tachyzoites in vacuoles were marked by using specific antibody of mouse anti-SAG1 staining by IFAT at 24 or 32 h post-infection and then counted in at least 100 vacuoles. All assays of this experiment were developed in triplicate and repeated at least three times.

Egress assay

Vero cells (1×10^5 per well) were used to plate on 12-well cultured for 24 h. Fresh purified tachyzoites (2×10^5 per well) were inoculated onto cell monolayers for 32 h infection under normal growth conditions as described above. For HYD and CAR assay, infected cells were treated by 2-fold and 4-fold IC_{50} value of compounds for 10 min before incubating with 3 μM A23187. And next, the wells were fixed and IFAT was stained with *T. gondii* specific antibodies of mouse anti-SAG1 and rabbit anti-GRA7 to evaluate egressed PV rates. At least 300 vacuoles were counted per slip as described above. All assays were performed in this experiment in triplicate and repeated at least three times.

Treatment assay in mice model

Fresh tachyzoites were purified and counted as described above and then used to inject into 7-week-old female BALB/c mice by intraperitoneal injection. For treatment by HYD and CAR assay, at 24 hour post-infection, acute infected mice were intraperitoneally (i.p.) injected with the compounds at either, 5 and 20 mg/kg HYD, 10, 25 and 50 mg/kg CAR, or PBS for 7 days. Daily observations of mice were noted, such as body weight, morbidity, mortality and clinical signs. Surviving mice were monitored for 30 days and blood was drawn at day 30 to confirm infection using ELISA assay, as well as tissues were collected to determine parasite burdens through

targeting of *TgB1* gene by quantitative PCR (qPCR). GraphPad Prism 7 (GraphPad Software Inc., La Jolla, CA, USA) was used to graph cumulative mortality as Kaplan–Meier survival plots and analyzed.

DNA isolation and quantitative PCR (qPCR) detection of *T. gondii*

DNA was extracted from the brains of HYD, CAR or PBS-treated surviving mouse on day 30 by DNeasy Blood & Tissue Kit (QIAGEN, Germany), according to the manufacturer's instructions. The brain DNA was then amplified with specific primers targeting to the *B1* gene of *T. gondii*. In the present study, the standard curve was constructed by using 10-fold serial dilutions of *T. gondii* DNA extracted from 10^5 *T. gondii* tachyzoites; thus, the curve ranged from 0.01 to 10,000 parasites, as above. The parasite burdon was counted by using this generated standard curve. Likewise, DNA was extracted from the 2×10^7 tachyzoites treated with 0.25-fold, 0.5-fold and 1-fold IC_{50} values of HYD and CAR or sulfadiazine (1 mg/ml). DNA from each tachyzoite sample (30 ng) which were treated with 1/4, 1/2 and IC_{50} concentration of HYD and CAR were used to amplify fragments of *Toxoplasma* mitochondrial genome cytochrome b (*CytB*) (forward primer 5'- TAC CGC TTG GAT GTC TGG TT -3', the reverse primer 5'- AAC CTC CAA GTA GCC AAG GT -3') and apicoplast genome elongation factor Tu (*EF-Tu*) (forward primer 5'- TGT GCT CCT GAA GAA ATA GC -3', the reverse primer 5'- CAT TGG CCC ATC TAC AGC AG -3'), respectively, as previously described (Korsinczky et al., 2000; Uddin et al., 2018). The expression levels of target genes were normalized to *Tg β-tubulin* (forward primer 5'- CAC TGG TAC ACG GGT GAA GGT -3', the reverse primer 5'- ATT CTC CCT CTT CCT CTG CG -3') mRNA levels using the $2^{\Delta\Delta Ct}$ method. The amplification, data acquisition, and data analysis were carried out in the ABI Prism 7900HT Sequence

Detection System (Applied Biosystems, USA), and the cycle threshold values (C_t) were calculated as described above.

Statistical analysis

The GraphPad Prism 7 software (GraphPad Software Inc., USA) was used in this study to graph and analyze the results. The statistical analyses were developed in the present study by an unpaired Student's *t*-test, Chi-squre Test, Tukey's Multiple Comparison Test, and one-way ANOVA plus Tukey-Kramer *post hoc* analysis. For the survival curves, the Kaplan-Meier method and statistical comparisons were developed by the log-rank method. Data represent the mean ± Standard Error of Mean. A p value < 0.05 was considered statistically significant.

3-3. Results

HYD and CAR inhibit *T. gondii* growth *in vitro*

First, the toxicity of HYD and CAR on host cells *in vitro* was analyzed using the CCK-8 cell counting kit. HFF cells were exposed to 100 μg/ml of HYD for 24 h, and then the rate of cell proliferation was 109.02%, while when exposed to 200 μg/ml of HYD, the proliferation rate of HFF cells was fall to 54.51% (Fig. 13A). The cytotoxic 50% inhibitory concentration (IC_{50}) value was determined as 210.2 μg/ml (Fig. 13B). However, when HFF cells were treated with CAR even at a high concentration of 1000 μg/ml, the proliferation rate was over 95.89% (Fig. 13A). Therefore, the safe concentration of compounds for HFF cell was considered to be < 100 μg/ml (HYD) and 1000 μg/ml (CAR) in this study, respectively. For Vero cells exposed to 200 μg/ml of HYD, the proliferation rate was 101.11% while exposed to 400 μg/ml was only 6.94% (Fig. 13C). The IC_{50} value of HYD against Vero cells was 296.6 μg/ml

(Fig. 13D). A proliferation rate of 97.78% was noted on Vero cells treated with 1000 μg/ml CAR (Fig. 13C). Therefore, the safe concentration of compounds for Vero cells were considered to be < 200 μg/ml HYD and 1000 μg/ml CAR in this study, respectively.

To evaluate the potential of anti-*Toxoplasma* of compounds *in vitro*, the fluorescence intensity of RH-GFP on HFF cells was examined after treatment with HYD, CAR, DMSO (negative control) and sulfadiazine (positive control). RH-GFP parasite growth was inhibited by 50 μg/ml CAR with little fluorescence (Fig. 13E), while the GFP signal was still detected even at the highest concentration of sulfadiazine (1 mg/ml). Both compounds were able to inhibit parasite growth, with the IC_{50} values of 4.286 μg/ml of HYD and 23.11 μg/ml of CAR on RH-GFP (Fig. 13F and G). Meanwhile, selectivity indices (SI) of HYD and CAR for RH-GFP on HFF cells was 49.04 and > 43.27, respectively.

T. gondii* lytic cycle is impaired by HYD and CAR *in vitro

T. gondii lytic cycle starts from the energy-dependent extracellular tachyzoite invasion into host cells, followed by the rapid intracellular tachyzoite replication, egress, and reinvasion of neighboring cells (Nitzsche et al., 2016). Studies on plaque formation can result the complete rounds of *T. gondii* lytic cycle *in vitro* (Lourido et al., 2012; Shen and Sibley, 2014). Therefore, to analyze the effects of HYD and CAR on the lytic cycle of *T. gondii*, two-fold or four-fold IC_{50} values of either of the compounds were used to perform attachment and invasion, replication and egress assays on Vero cells, as well as two fold IC_{50} values of compounds were used to conduct plaque formation assay on HFF cells.

For parasite invasion, two-fold IC_{50} values of HYD or CAR decreased the percentage of invaded parasites, although non-significant. Remarkably, when treated by 4-fold of the IC_{50} values, the invasion was significantly reduced by 46.03% in HYD and 43.36% in CAR, whereas just 12.41% reduction of tachyzoite invasion was determined even at the high concentration of sulfadiazine (1 mg/ml) treatment (Fig. 14A).

To determine the effects of HYD and CAR on intracellular replication *in vitro*, Vero cells were infected with fresh tachyzoites for 24 h in presence of 2-fold or 4-fold IC_{50} values of either of the compounds and 1 mg/ml sulfadiazine. Parasite replication was impaired when treated with 2-fold IC_{50} values of HYD or CAR, and replication was almost completely abolished by treatment with 4-fold IC_{50} values of the compounds (Fig. 14B and C). Notably, HYD showed a stronger inhibitory effect than CAR.

For the egress assay, both HYD and CAR pretreatment significantly decreased the egressed rate compared to DMSO pretreatment (Fig. 14D), suggesting that the ability of tachzoite egress from host cells was impaired.

Furthermore, a plaque assay was conducted to observe the complete round of lytic cycle (Fig. 14E). In the presence of HYD or CAR, parasites formed smaller plaque sizes with less plaque numbers than DMSO treatment (Fig. 14F and G). These results suggested that *T. gondii* lytic cycle is impaired by HYD and CAR *in vitro*.

Treatment with the HYD and CAR control acute toxoplasmosis in the mice

To assess the inhibitory effects of compounds on *T. gondii in vivo*, female BALB/c mice were injected intraperitoneally (i.p.) with an acute dose of 5×10^4 type II PLK strain tachyzoites and treated by i.p. with 5 or 20 mg/kg of body weight HYD, 10, 25 or 50 mg/kg of body weight CAR, or PBS once daily from day 1 to day 7 post-

infection. Body weight, clinical signs, and survival rates were recorded. As expected, treatment with 20 mg/kg HYD and 10 mg/kg CAR significantly increased survival rate during acute infection with slight body weight reduction and lower clinical scores compared to PBS treatment (Fig. 15A, B and C). However, the higher clinical scores were seen in the 25 and 50 mg/kg CAR-injected mice from 2 days post infection (dpi). Moreover, 50 mg/kg CAR-treated mice died at 7 and 8 dpi, earlier than PBS, suggesting that although CAR can control acute toxoplasmosis, high concentrations can be toxic to mice. On the other hand, the parasite burdens in survival mice brain tissues were examined by qPCR, where I observed significantly lower loads on HYD and CAR treated brains than PBS (Fig. 15D). Collectively, HYD and CAR treatment controlled acute *T. gondii* infection in mice model, although parasites were detected in brains.

HYD and CAR inhibit *T. gondii* growth through an AAT-independent pathway

The aforementioned results revealed that HYD and CAR controlled acute *T. gondii* infection in mice, however, *AAT*-deficiency did not abolish the virulence of PLK or RH *in vivo*. Therefore, HYD and CAR might inhibit *T. gondii* growth through *AAT*-independent pathway. To evaluate this, *AAT*-deleted parasite was treated with either HYD or CAR to determine extracellular invasion and intracellular replication of parasites. The result showed that treatment with as high as 4-fold of IC_{50} values of HYD and CAR, invasion rates of mutant parasites were not significantly different among HYD, CAR and DMSO, compared to the wild-type and complemented invasion rates (Fig. 16A and B). Interestingly, as presumed, intracellular replication of *AAT*-deficient parasites was also slowed down by both 2-fold and 4-fold IC_{50} values of HYD and CAR, compared to parental parasites (Fig. 16C). On the other hand, above mentioned showed that α-ketoglutarate supplementation significantly rescued

defects due to loss of *AAT*, so whether HYD- or CAR-impaired growth can be rescued by α-ketoglutarate was also determined. The experiment revealed that presence of α-ketoglutarate in HYD- or CAR-treated RH-infected cells slightly increased parasite replication (Fig. 16D). Altogether, HYD and CAR inhibit *T. gondii* growth that is largely independent of AAT pathway. Further, using 0.25, 0.5 or 1-fold IC_{50} concentration of HYD and CAR to treat RH parasite growth for 5 days, showed that relative transcription level of mitochondrial genome (*CytB* gene) was reduced followed increasing compounds (Fig. 16E), suggesting that compounds impaired parasite lytic cycle may relate to mitochondria function.

3-4. Discussion

The present studies reveal that HYD and CAR inhibited *T. gondii* growth by impairing the rounds of lytic cycle, including inactivated extracellular invasion or reinvasion, slowed intracellular replication and inhibited egress resulting in unformed plaques. Importantly, HYD and CAR also had anti-*Toxoplasma* activity *in vivo*. As for the inhibition of asexual stages, it is not surprising that acute infection of *T. gondii* was controlled by both compounds in mice.

A previous study reports that parasitic IC_{50} value of sulfadiazine anti-*T. gondii* type I parasites (RH strain) on HFF cell was 70 μg/ml (de Oliveira et al., 2009). However, lower IC_{50} values of HYD (4.286 μg/ml) and CAR (23.11 μg/ml) on type I RH-GFP strain in HFF cells were obtained in the present study. Regarding pyrimethamine, this study did not test the effects due to the currently used RH-GFP parasites which have the pyrimethamine-resistant gene (*DHFR*) (Nishikawa et al., 2003; Nishikawa et al., 2008; Leesombun et al., 2020). However, a published study reveals that IC_{50} value of

pyrimethamine against *T. gondii* is 0.84 μg/ml, and an SI value of more than 11.9 (Abugri et al., 2018). Obtained IC_{50}s of HYD and CAR on type I strain (RH-GFP) are between the values of sulfadiazine and pyrimethamine, and current results examined the high selectivity indices of 49.04 and more than 43.27 against *T. gondii*, confirming that HYD and CAR should be safe and efficient at inhibiting the growth of *T. gondii*.

It has been reported that HYD and CAR inhibited AAT activity in *P. falciparum* which is responsible for the reversible reaction of aspartate and α-ketoglutarate into oxaloacetate and glutamate (Berger et al., 2001; Wrenger et al., 2011). Compared with the above study, although the reaction of transamination of r*Tg*AAT, which catalyzes aspartate and α-ketoglutarate to glutamate, was inhibited by HYD and CAR treatments, more than 10-fold differences in IC_{50} values of HYD or CAR against cultured type I *T. gondii* parasites versus r*Tg*RHAAT enzyme was recorded. This weakens the argument that these compounds inhibited *T. gondii* parasites by targeting *AAT*. Current findings are in contrast to a previous work in *P. falciparum* which displayed a parasitic IC_{50} value in the same range that of HYD for the r*Pf*AAT enzyme *in vitro* (Wrenger et al., 2011). *TgAAT*s are distantly related to the predicted *P. falciparum AATs* with a relatively low 33% identity, thus it is possible that the AATs in two apicomplexan parasites have different functions and different sites of drug action may occur. In a previous study, Berger et al. (2001) found that AATs also play a role in the final step of methionine regeneration from methylthioadenosine in parasitic protozoa, but since this reaction is dependent on transamination, it was not investigated in the current study.

As expected, current results confirm that deficiency of *AAT* both in RH and PLK inhibited the parasite ability of invasion, replication, egress and plaque formation *in*

vitro consistent with the inhibition of *T. gondii* lytic cycle by HYD and CAR, although loss of *AAT* did not completely abolish parasite growth. However, the intracellular replication of *AAT*-deficient parasites was inhibited with HYD or CAR similar to parental parasites. This suggests that another pathway might be the target of these compounds. HYD and CAR treatment did not significantly slow down invasion rates of mutant parasites compared to parental parasites, which may imply that compounds have slight activity for inhibition of invasion by AAT reaction, consistent with the current catalytic inhibitors assay. Collectively, HYD and CAR inhibit parasite growth largely through other substrates in *T. gondii*.

However, although the growth defect due to loss of *AAT* was significantly rescued by treatment with α-ketoglutarate, current data show that the impaired replication caused by HYD and CAR treatment was not rescued through α-ketoglutarate supplementation. These denote that the inhibition activity of HYD and CAR may not be because of the association of α-ketoglutarate mechanism to AAT or other metabolic enzymes of α-ketoglutarate pathway (MacRae et al., 2012; Jacot et al., 2016). Additionally, this impairment of α-ketoglutarate homeostasis in *T. gondii* by loss of *AAT* enhanced the PLK parasitic virulence *in vivo*. Therefore, I doubt whether α-ketoglutarate re-uptake affects the virulence of type II PLK parasites *in vivo*, and assume that the metabolic enzymes directly related to α-ketoglutarate uptake may not effective drug targets against *T. gondii*. Overall, the current data suggest that control of parasite growth by HYD and CAR is not a result of the inhibition of α-ketoglutarate pathway on *T. gondii in vitro* and *in vivo*. Taken together, all these indicated that HYD and CAR inhibiting *T. gondii* growth and controlling toxoplasmosis can occur in an AAT-independent pathway.

3-5. Summary

In summary, *T. gondii* is an obligate intracellular protozoan parasite and a successful parasitic pathogen in diverse organisms and host cell types. Hydroxylamine and carboxymethoxylamine have been reported as inhibitors of *AAT*s, and interferes with the proliferation in *P. falciparum*. Therefore, *AAT*s are suggested as drug targets against *Plasmodium*. *T. gondii* genome encodes only one predicted *AAT* in both *T. gondii* type I RH and type II PLK strains. However, effects of HYD and CAR, and their relationship with AAT on *T. gondii* remain unclear. In this study, the results revealed that HYD and CAR impaired the lytic cycle of *T. gondii in vitro*, including the inhibition of invasion or reinvasion, intracellular replication and egress. Importantly, HYD and CAR had the ability of controlling acute toxoplasmosis *in vivo*. Further studies showed that HYD and CAR could inhibit the transamination activity of r*Tg*AAT *in vitro.* However, the results confirmed that deficiency of *AAT* in both RH and PLK did not reduce the virulence in mice, although the growth ability of the parasites was affected *in vitro*. HYD and CAR could still inhibit the growth of *AAT*-deficient parasites. All these indicated that HYD and CAR inhibiting *T. gondii* growth and controlling toxoplasmosis can occur in an AAT-independent pathway. Overall, further studies focusing on the elucidation of the mechanism of inhibition is warranted. This study hints at new substrates of HYD and CAR as potential drug targets to inhibit *T. gondii* growth.

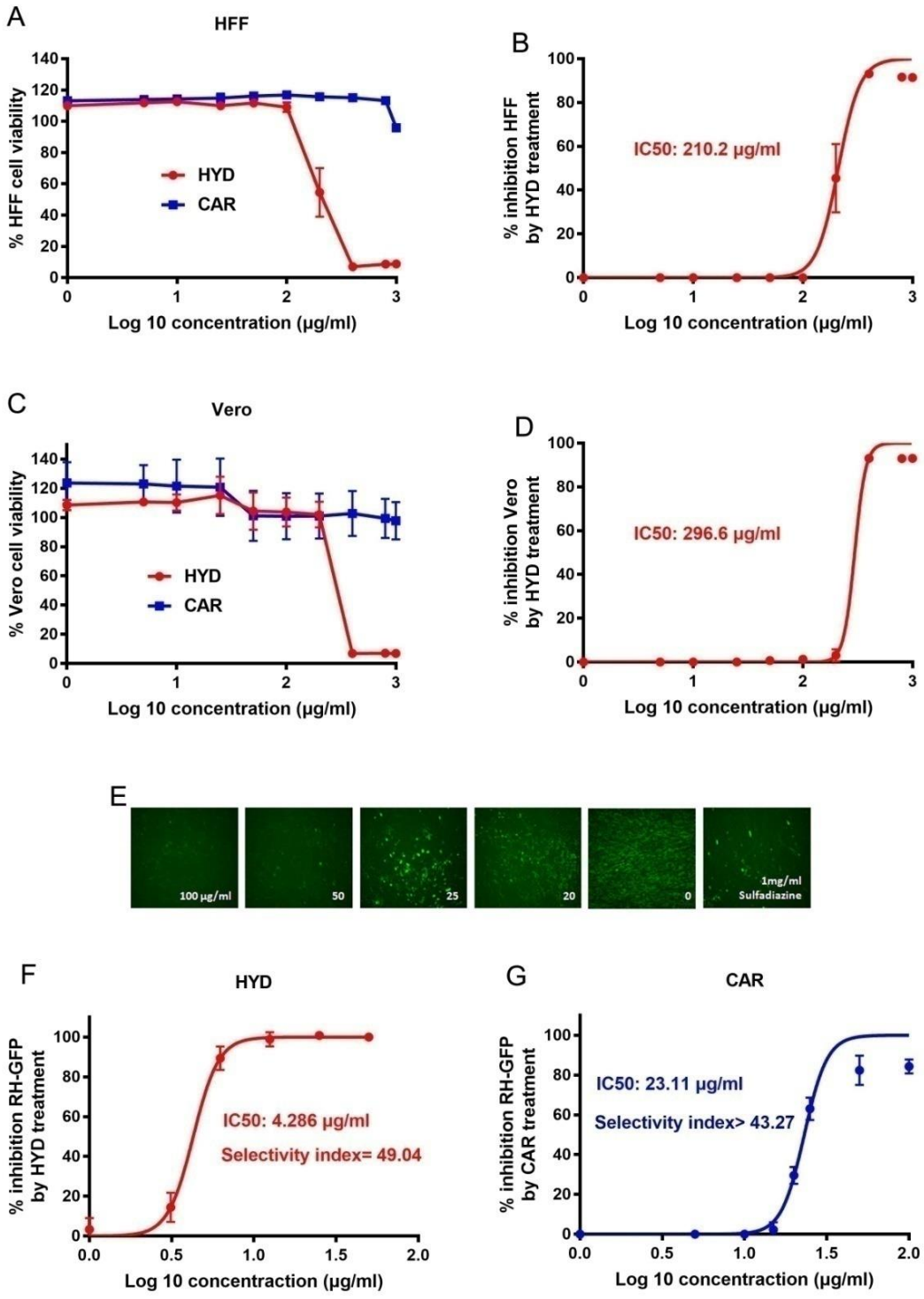

Fig. 13. HYD and CAR inhibit *T. gondii* growth *in vitro*. (A) HFF cell viability treated with HYD and CAR. (B) Inhibition of HFF growth with HYD treatment. The

50% inhibitory concentration was examined. (C) Vero cell viability treated with HYD and CAR. (D) Inhibition of Vero cell growth by HYD treatment. (E) The fluorescence intensity of RH-GFP on HFF cells after treatment with increasing concentration of CAR or sulfadiazine. (F and G) Inhibition of RH-GFP parasites after HYD (F) and CAR (G) treatment. IC_{50} and selectivity index were determined.

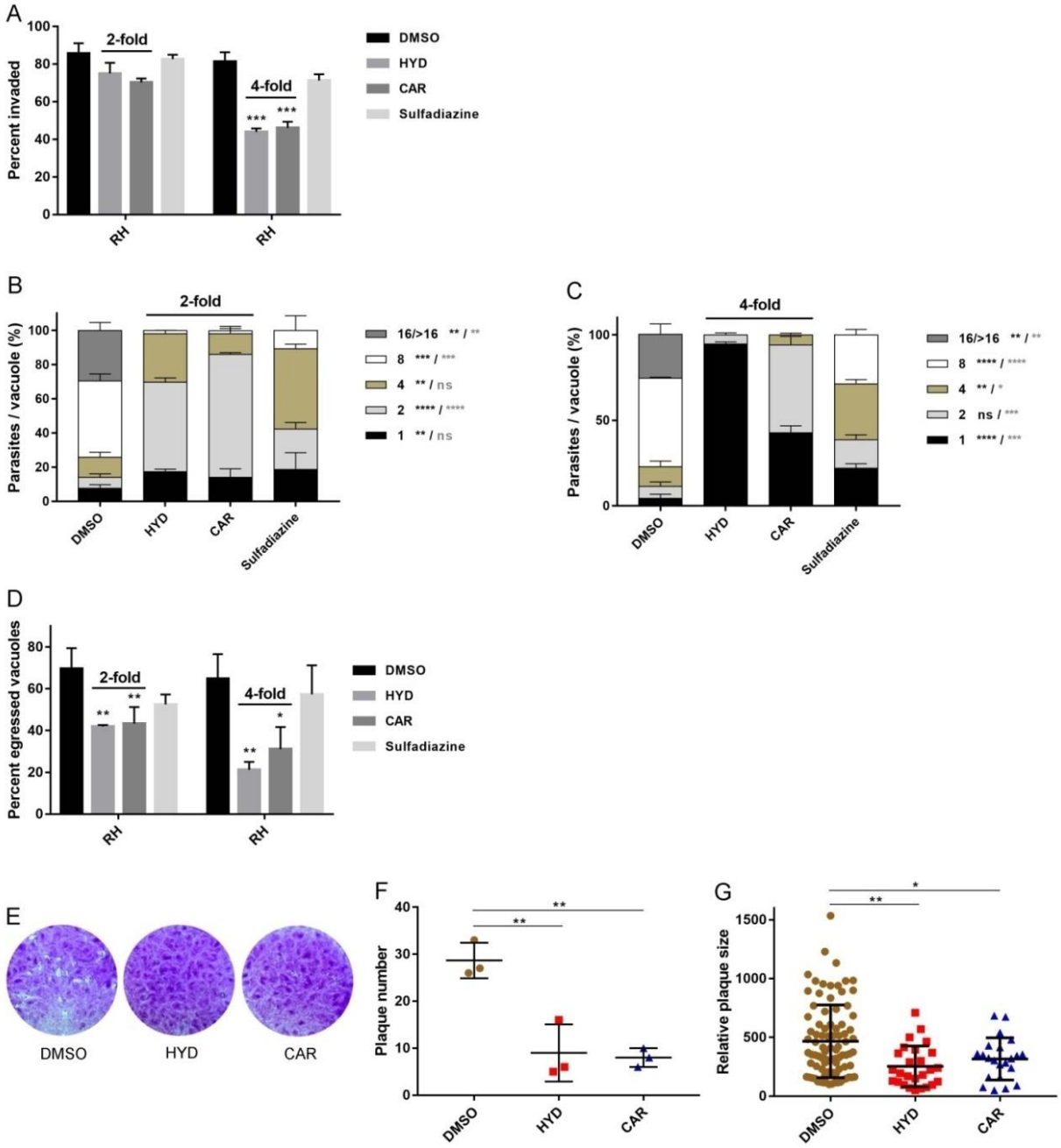

Fig. 14. *T. gondii* lytic cycle is impaired by HYD and CAR *in vitro*. (A) Invasion assay. Purified tachyzoites were pretreated with either of the two compounds of 2-fold or 4-fold IC_{50} values, sulfadiazine (1 mg/ml), or DMSO for 1 h at 37 ℃, then allowed invasion for 2 h, and dual staining to determine the percentage of invaded parasites. (B and C) Intracellular replication assay. HYD and CAR of 2-fold (B) or 4-fold (C)

IC_{50} values were allowed to treat infected RH parasites for 24 h, and the number of parasites in 100 random vacuoles was counted and plotted. (D) Egress assay. Infected cells were treated with compounds of 2-fold and 4-fold IC_{50} values for 10 min before incubating with 3 μM A23187. After incubation, mouse anti-SAG1 and rabbit anti-GRA7 were used to determine the rate of staining egressed PVs. The vacuoles of at least 300 were counted each slip. (E) Plaque formation assay. Fresh 150 tachyzoites of RH strain were used to infect HFF cell monolayer, and allowed to grow for 8 days with HYD or CAR of 2-fold IC_{50} value, and then 0.1% crystal violet was used to stain. (F and G) Relative plaque number (F) and plaque size (G) in panel D. The data are presented as the mean ± SEM of at least three independent experiments. * $p < 0.05$, ** $p < 0.01$, *** $p < 0.001$, **** $p < 0.0001$, compared with DMSO treatment, determined by Chi-square Test (invasion and egress assay), Tukey's Multiple Comparison Test (replication assay, deep asterisk stands for HYD vs. vehicle, and light asterisk stands for CAR vs. vehicle) and one-way ANOVA plus Tukey-Kramer *post hoc* analysis (plaque assay).

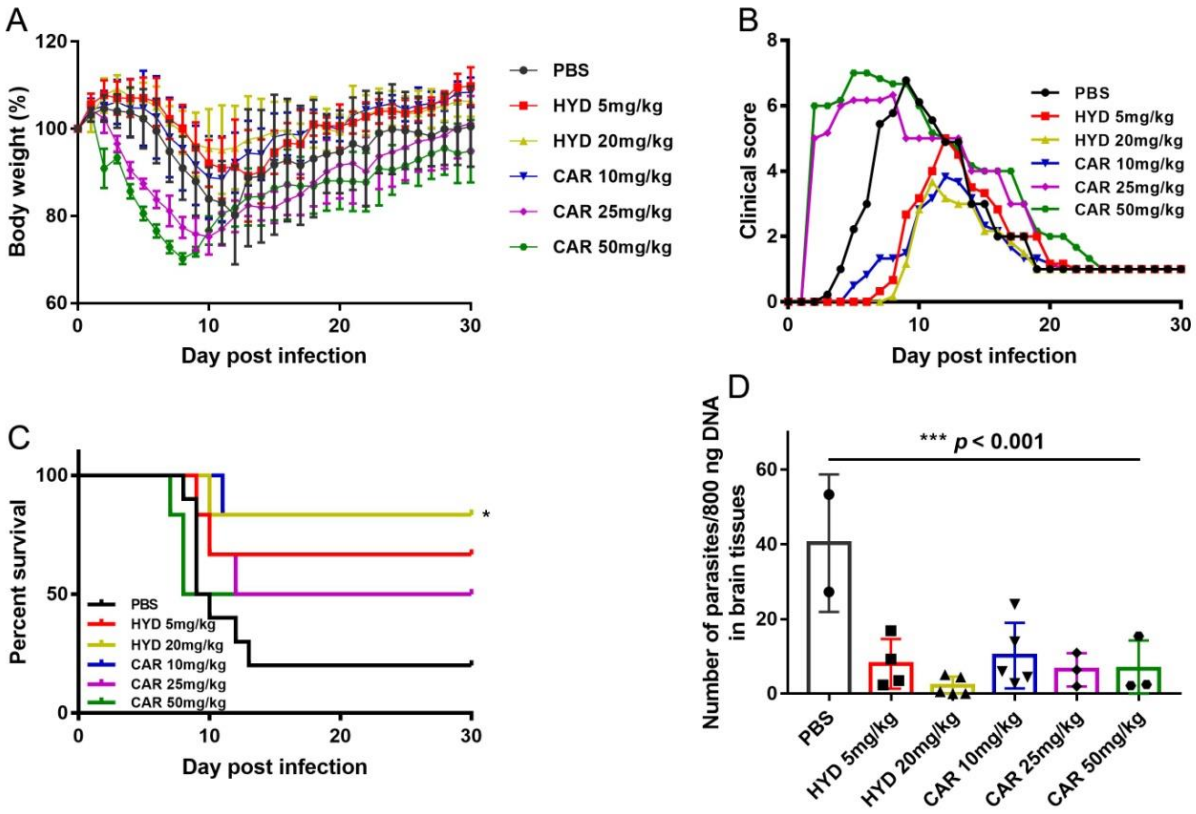

Fig. 15. HYD and CAR control acute *T. gondii* infection in mice. Female BALB/c mice were infected by i.p. with an acute dose of 50,000 PLK tachyzoites and treated by i.p. from day 1 to day 7 post-infection with 5 and 20 mg/kg HYD, 10, 25 and 50 mg/kg CAR, or PBS once daily, and body weight, morbidity, mortality and clinical signs were noted. (A) Body weight %. (B) Mean clinical scores. The scores varied from 0 (no signs) to 10 (all signs). (C) Survival rates. * $p < 0.05$, Log-rank (Mantel-Cox) test. (D) Parasite burdens of survival mice brains. At day 30 post-infection, the brains were collected and DNA was extracted, 800 ng DNA was used to detect the number of parasites. *** $p < 0.001$, one-way ANOVA plus Tukey-Kramer *post hoc* analysis.

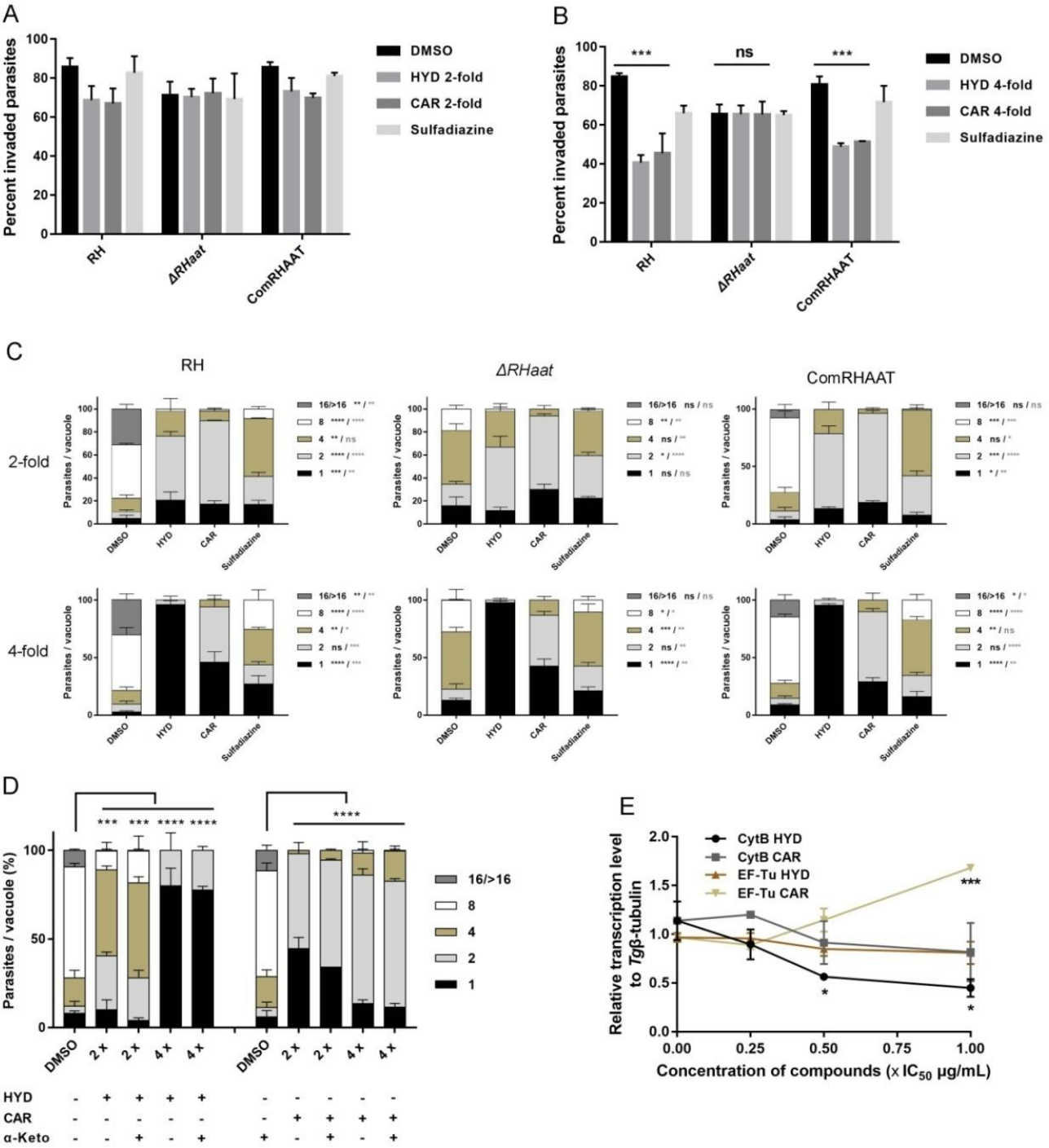

Fig. 16. HYD and CAR inhibit *T. gondii* growth through AAT-independent pathway. (A and B) Effects of *AAT*-deficient parasite invasion treated with HYD and CAR compared with parental and complemented. Data shows the mean ± SEM of three independent experiments. *** $p < 0.001$, determined by Chi-square Test. (C) Effects

of HYD and CAR treatment for *AAT*-deficient parasite replication. The 2-fold or 4-fold of IC_{50} values of HYD and CAR were used to treat three strains parasites replication. * $p < 0.05$, ** $p < 0.01$, *** $p < 0.001$, **** $p < 0.0001$, deep asterisk stands for HYD vs. vehicle, light asterisk stands for CAR vs. vehicle, determined by Tukey's Multiple Comparison Test. (D) α-ketoglutarate (α-Keto) assay. α-ketoglutarate supplementd to the HYD and CAR treatment medium, and then replication was determined at 24 h post-infection. *** $p < 0.001$, **** $p < 0.0001$, determined by Tukey's Multiple Comparison Test. (E) Effects of HYD and CAR on mitochondrial genome and apicoplast genome. The 2×10^7 tachyzoites were treated by 0.25-fold, 0.5-fold and 1-fold of IC_{50} values of HYD and CAR, or sulfadiazine (1 mg/ml) for 5 days, to investigate the expression of *CytB* and *EF-Tu* gene by qPCR. * $p < 0.05$, *** $p < 0.001$, one-way ANOVA plus Dunnett's multiple comparisons test.

General discussion

Toxoplasma gondii lytic cycle starts from the invasion of extracellular tachyzoite into host cells, and following intracellular tachyzoite replication, egress from the cells, and reinvasion of neighboring cells (Nitzsche et al., 2016). This parasite needs to develop the carbon metabolism for survival in the tachyzoite stage, such as glycolysis, tricarboxylic acid (TCA) cycle, gluconeogenesis, and pentose phosphate shunt (Kissinger et al., 2003; Fleige et al., 2007; Fleige et al., 2008). Although the carbon sources are largely different in various stages of *T. gondii* development, the glucose and glutamine can both be utilized as carbon sources while either glucose or glutamine is sufficient to guarantee *T. gondii* survival (MacRae et al., 2012; Blume et al., 2015; Nitzsche et al., 2016). Previous studies have reported how glucose-derived carbon enters the mitochondrial TCA cycle and some metabolic enzymes play critical roles for intermediate homeostasis, parasite growth and virulence as judged by stable isotope labelling, metabolomic analysis and genome editing (Blume et al., 2009; MacRae et al., 2012; Blume et al., 2015; Shukla et al., 2018; Xia et al., 2018a; Xia et al., 2019). Several studies also found that in *T. gondii*, glutamine, which can enter the mitochondria by glutaminolysis, can be utilized as carbon skeletons to the TCA cycle either via the conversion of intermediate glutamate to α-ketoglutarate or via the GABA shunt (Blume et al., 2009; MacRae et al., 2012). Additionally, some studies showed that the enzymes in these pathways also contribute to the virulence of parasites and could be used as potential drug targets for toxoplasmosis treatment (MacRae et al., 2012; Oppenheim et al., 2014; Xia et al., 2018a; Xia et al., 2019)

This study focused on the glutamine pathway in the conversion of intermediate glutamate to α-ketoglutarate in glutaminolysis. *T. gondii* genome contains three enzymes which allow speculation on the possible architecture of the pathway, the aspartate aminotransferase (*AAT*), glutamate dehydrogenases (*GDHs*) and alanine transaminase (*AlAAT*) (Jacot et al., 2016). Here, *AAT* gene, was chosen, as this has been reported to be a drug target against *Plasmodium*. Further studies were developed to perform functional analysis on this predicted enzyme in both *T. gondii* type I RH and type II PLK strains, and to assess the potentials of reported inhibitors of AATs for treating toxoplasmosis, as well as their relationship with *Tg*AAT.

The results showed that the recombinant *Tg*AAT protein could use the L-aspartate as a substrate, which was determined according to the previous methods (Wrenger et al., 2011; Wrenger et al., 2012). This is consistent with expected result and the transamination activity in *Plasmodium* rAAT (Wrenger et al., 2011; Wrenger et al., 2012; Jacot et al., 2016), wherein the *T. gondii* rAAT catalyzes the reversible conversion of oxaloacetate and glutamate to aspartate and α-ketoglutarate. Further study indicates that although loss of *AAT* in RH and PLK strains significantly reduced parasite growth *in vitro*, *AAT* is not essential to the parasite growth under optimal culture conditions. Importantly, α-ketoglutarate supplementation could rescue the growth defect in *AAT*-deleted parasites, suggesting that it plays an important role at least in α-ketoglutarate metabolism of glutamine pathway which is consistent with the expectations. Regrettably, the results showed different phenotypes of PLK *AAT*-deleted mutants between *in vivo* and *in vitro*. Although loss of *AAT* in PLK parasite significantly decreased parasite growth *in vitro*, the *AAT*-deficient mutant parasites did not abolish acute virulence but even enhanced the virulence as observed in BALB/c mice. These unexpected results brought me to consider whether the cultured

parasites under different *in vitro* and *in vivo* conditions, such as different α-ketoglutarate concentrations, resulted in different phenotypes of deleted *AAT* parasites *in vitro* and *in vivo*.

On the other hand, the current data revealed that hydroxylamine (HYD) and carboxymethoxylamine (CAR), reported inhibitors of AATs, controlled acute toxoplasmosis in mice and inhibited *T. gondii* growth *in vitro*, but two compounds remains to inhibit the replication of *AAT* deleted parasites *in vitro*. Hence, HYD and CAR might be acting on *T. gondii* through a manner independent of the AAT pathway *in vitro* and *in vivo*, and instead in another pathway. The fact that α-ketoglutarate supplementation did not rescue the growth inhibitions caused by HYD and CAR, indicates that HYD and CAR are not results of the inhibition of α-ketoglutarate pathway. Interestingly, these two compounds exhibited similar inhibitory activities in different tests, which may be because of the hydroxylamine unit in the structure of CAR. Hydroxylamine and its compounds have the potential to inhibit the activity of some enzymes in viruses, bacteria, fungi, and protozoa (Gross, 1985; Sarojini and Oliver, 1985). Importantly, the current study revealed that HYD and CAR impairment of the parasite lytic cycle may be associated with the inhibition of mitochondria function of α-ketoglutarate-independent pathway (Korsinczky et al., 2000; Uddin et al., 2018). However, further studies focusing on the elucidation of the mechanism of inhibition is warranted. The present study hints at new substrates of HYD and CAR as potential drug targets to inhibit *T. gondii* growth.

In this study, the *AAT* gene was identified and analyzed in *T. gondii* using gene-deficient strains, and two inhibitors were tested as effective and safe compounds for controlling toxoplasmosis. However, this study still has some unsolved queries: (1) although the current study proves that AAT may be involved largely in the α-

ketoglutarate pathway, other pathways may also be involved in the growth reduction of *T. gondii* parasites caused by *AAT* deletion; (2) why do the *AAT*-deficient strains showed faster replication than wild-type infection *in vivo*? Because this study found that a high concentration of α-ketoglutarate caused the growth of mutant parasites faster *in vitro*, could it be that the high concentration of α-ketoglutarate nutrients in animals explains this finding *in vivo*? (3) this research determined the safety and effectiveness of HYD and CAR in inhibiting the growth of *T. gondii*, however, they don't seem to depend only on a specific pathway, AAT, to develop inhibition. Overall, future research is needed to explain these scientific problems.

General summary

Toxoplasma gondii is a protozoan parasite of which cats are the final host and humans or other animals are the intermediate hosts. Toxoplasmosis, caused by *T. gondii*, is an important zoonotic disease spreading worldwide, that threatens human health and causes economic losses in livestock industry. However, there is no effective vaccine, and a combination of compounds, pyrimethamine and sulfadiazine, is commonly used for treatment, but there are concerns about side effects and drug resistance problems. Hence, there is a strong demand for the development of safer and more effective therapeutic drugs. In this study, the function of aspartate aminotransferase (AAT) of *T. gondii* was analyzed, and the potentials of reported inhibitors of AATs for treating toxoplasmosis were assessed.

In chapter 1, *AAT* gene was characterized in *T. gondii* type I RH and type II PLK strains. The results showed that *TgAAT*s were 1,794 bp nucleotide sequences coding 597 amino acid sequences. The sequencing analysis indicated that *Tg*AAT has distant identities of 46% with that in *Homo sapiens* and *Mus musculus*. Furthermore, the ability of r*Tg*AAT for using the L-aspartate and α-ketoglutarate as the substrates in the transamination reaction was confirmed and this is consistent with the predictions and with the results in *Plasmodium*. Importantly, two compounds, hydroxylamine (HYD) and carboxymethoxylamine (CAR), known as AATs inhibitors were found that they could indeed inhibit the activity of this enzyme. These data suggest that these two compounds could have potential to inhibit the growth of *T. gondii* through the pathway of AAT, but it remains to be confirmed by further experiments.

In chapter 2, the deficient lines of the *AAT* gene in *T. gondii* type I RH and type II PLK strains were generated and characterized. The *AAT* genes were identified from the *T. gondii* genome database, and the deficient strains (*Δaat*s) targeted were developed using the CRISPR/Cas9 genome-editing system. In addition, the functionally complemented strains (ComAATs) in which *AAT* was restored were also prepared. Through a series of experiments, data demonstrated that the *AAT* gene was deleted as expected in the *TgΔaat* strains, and that the *AAT* gene was restored as expected in the ComAAT strains. Furthermore, the functions of the *AAT* gene were identified by comparing with wild-type strains, *Δaat* strains, and ComAAT strains. Results showed that *AAT* gene-deficient parasites had a markedly reduced growth rate *in vitro* compared with the wild-types, and this growth damage in *Δaat* lines was restored by reversion to *AAT*. Importantly, this study found that the defect of growth caused by loss of *AAT* could be rescued by supplementary α-ketoglutarate, suggesting that AAT plays a role in α-ketoglutarate metabolism in *T. gondii*. On the other hand, no significant reduction was observed in the pathogenicity of *AAT* gene-deficient strains *in vivo*. Overall, these results suggest that the metabolic system controlled by AAT plays an important role in the *in vitro* growth of parasites.

In chapter 3, the inhibitory effects of HYD and CAR, were investigated on the growth of wild-type strains. This study found that HYD and CAR impaired the lytic cycle of *T. gondii in vitro*, and had the ability to control acute toxoplasmosis *in vivo*. However, even in *AAT* gene-deficient parasites, these growth-inhibitory effects were not significantly attenuated, suggesting that the inhibitory actions of HYD and CAR are AAT-independent. In the future, it will be required to search for other inhibitors of AAT and to elucidate the anti-*T. gondii* mechanisms of HYD and CAR.

In summary, the *AAT* gene was identified for the first time in *T. gondii* and its function was analyzed using gene-editing system, and that *AAT* plays an important role in the growth of parasites. On the other hand, the current data suggest that HYD and CAR can be safe and effective drug candidates for inhibiting the growth of *T. gondii*. Further studies targeting the mechanisms of action of HYD or CAR are warranted, which is expected to contribute to the development of new therapeutic methods for toxoplasmosis.

和文要約

トキソプラズマは、ネコ科動物を終宿主とし、ヒトや他の動物を中間動物とする原虫である。この原虫の感染を起因とするトキソプラズマ症、世界中広く分布している人獣共通感染症であり、ヒトの健康や動物生産に危害を及ぼす。今のところトキソプラズマ症に対する有効なワクチンはなく、ピリメタミンとサルファ剤の併用による治療法が一般的である。しかし、この治療法には副作用や薬剤耐性の問題が指摘されている。そこで、本研究では新規治療法開発を目的に、トキソプラズマのアスパラギン酸アミノ基転移酵素（AAT）の機能と AAT の酵素阻害剤の虫体増殖抑制効果について解析を行った。

第１章では、トキソプラズマのⅠ型 RH 株とⅡ型 PLK 株の *AAT* 遺伝子について分析した。*AAT* 遺伝子は 1794 塩基からなり、597 アミノ酸をコードすることが判明した。アミノ酸レベルで、ヒトやマウス由来の AAT とは 46%の相同性を示した。組換え *Tg*AAT は、予想通りアスパラギン酸を基質としたアミノ基転移反応を触媒し、マラリア原虫で得られた知見と一致した。さらに、AAT の酵素阻害剤として知られるヒドロキシルアミン（HYD）とカルボキシメトキシルアミン（CAR）は、組換え *Tg*AAT の酵素活性を阻害することを証明した。これらの結果より、HYD と CAR はトキソプラズマ虫体の増殖を抑制する可能性が示唆された。

第２章では、トキソプラズマ虫体における *AAT* 遺伝子の機能解析を行った。CRISPR/Cas9 を用いたゲノム編集法により、*AAT* 遺伝子欠損株と *AAT* 復帰し

た株をそれぞれ作製した。*AAT* 欠損株は、試験管内培養において野生型と比較し、その増殖性が著しく低下した。この増殖性の低下は、*AAT* 遺伝子復帰株では完全に回復した。また、*AAT* 欠損株の増殖性の低下は、α-ケトグルタル酸の添加により回復した。一方、*AAT* 欠損株はマウスの体内においては、野生型と比較し虫体の増殖性に顕著な低下は認められなかった。これらの結果により、AAT が司る代謝経路はトキソプラズマの試験管内増殖において重要な役割を果たすことが示唆された。

第３章では、AAT の酵素阻害剤である HYD と CAR の虫体増殖抑制作用を調べた。両阻害剤とも、試験管内において虫体の増殖を抑制した。また、マウス体内においても虫体の増殖を顕著に抑制した。しかしながら、*AAT* 遺伝子欠損株においても、これらの原虫増殖抑制作用が顕著に減弱しないことから、HYD と CAR のトキソプラズマ増殖抑制作用は、AAT 非依存的であることが示唆された。今後、AAT の他の阻害剤の探索や HYD と CAR の作用機序の解明が必要である。

以上のように、本研究ではトキソプラズマの *AAT* を初めて特定し、ゲノム編集法を用いてその機能解析を行った。その結果、*AAT* はトキソプラズマの増殖に重要な役割を果たすことが判明した。また、AAT の酵素阻害剤である HYD と CAR はトキソプラズマの治療薬候補となり得ることが示唆された。今後は、HYD と CAR の作用機序のさらなる解明が求められる。

Acknowledgements

This research works were carried out at National Research Center for Protozoan Diseases, Obihiro University of Agriculture and Veterinary Medicine, and supported by grants from the Ministry of Education, Culture, Sports, Science, and Technology of Japan (MEXT).

Firstly, I would like to express my most heartfelt gratitude to my supervisor, Professor Xuenan Xuan, who gave me a precious opportunity to join the Research Unit for Host Defense Laboratory, National Research Center for Protozoan Diseases, Obihiro University of Agriculture and Veterinary Medicine, and took me into the world of scientific research and his guidance support me to complete the important doctoral stage in my life.

Secondly, I would like to say thanks to my co-advisors, Professor Yoshifumi Nishikawa, Professor Makoto Igarashi, for giving me valuable comments and suggestions during my research. And I also would like to thank my reviewers, Professor Shin-Ichiro Kawazu, Professor Haruko Ogawa, for giving me constructive suggestions in my research and thesis.

Thirdly, I thank Professor Liqing Ma (Qinghai University, China), Professor Bayin Chahan (Xinjiang Agriculture University, China) and Professor Honglin Jia (Chinese Academy of Agricultural Sciences, China) who gave me the suggestions for my study and for providing materials.

Finally, I deeply say grateful to all lab members of Research Unit for Host Defense for the help in my experiment, paper publication, and life. I also thank the support from all of the staff in National Research Center for Protozoan Diseases and Obihiro

University of Agriculture and Veterinary Medicine, and all people who helped me complete the doctoral course.

References

Abugri DA, Witola WH, Russell AE, Troy RM. 2018. *In vitro* activity of the interaction between taxifolin (dihydroquercetin) and pyrimethamine against *Toxoplasma gondii*. Chem Biol Drug Des. 91, 194-201.

Adeyemi OS, Atolani O, Awakan OJ, Olaolu TD, Nwonuma CO, Alejolowo O, Otohinoyi DA, Rotimi D, Owolabi A, Batiha GE. 2019. *In vitro* screening to identify anti-*Toxoplasma* compounds and in silico modeling for bioactivities and toxicity. Yale J Biol Med. 92, 369-383.

Alday PH, Doggett JS. 2017. Drugs in development for toxoplasmosis: advances, challenges, and current status. Drug Des Devel Ther. 11, 273-293.

Berger LC, Wilson J, Wood P, Berger BJ. 2001. Methionine regeneration and aspartate aminotransferase in parasitic protozoa. J Bacteriol. 183, 4421-4434.

Black MW, Boothroyd JC. 2000. Lytic cycle of *Toxoplasma gondii*. Microbiol Mol Biol Rev. 64, 607-623.

Blume M, Nitzsche R, Sternberg U, Gerlic M, Masters SL, Gupta N, McConville MJ. 2015. A *Toxoplasma gondii* gluconeogenic enzyme contributes to robust central carbon metabolism and is essential for replication and virulence. Cell Host Microbe. 18, 210-220.

Blume M, Rodriguez-Contreras D, Landfear S, Fleige T, Soldati-Favre D, Lucius R, Gupta N. 2009. Host-derived glucose and its transporter in the obligate intracellular pathogen *Toxoplasma gondii* are dispensable by glutaminolysis. Proc Natl Acad Sci USA. 106, 12998-13003.

Brun-Pascaud M, Chau F, Garry L, Jacobus D, Derouin F, Girard PM. 1996. Combination of PS-15, epiroprim, or pyrimethamine with dapsone in prophylaxis of *Toxoplasma gondii* and *Pneumocystis carinii* dual infection in a rat model. Antimicrob Agents Chemother. 40, 2067-2070.

Cardew EM, Verlinde CLMJ, Pohl E. 2018. The calcium-dependent protein kinase 1 from *Toxoplasma gondii* as target for structure-based drug design. Parasitology. 145, 210-218.

Dantas-Leite L, Urbina JA, de Souza W, Vommaro RC. 2004. Selective anti-*Toxoplasma gondii* activities of azasterols. Int J Antimicrob Agents. 23, 620-626.

de Oliveira TC, Silva DA, Rostkowska C, Bóda SR, Ferro EA, Magalhães PM, Mineo JR. 2009. *Toxoplasma gondii*: effects of *Artemisia annua* L. on susceptibility to infection in experimental models *in vitro* and *in vivo*. Exp Parasitol. 122, 233-241.

Dégbé M, Debierre-Grockiego F, Tété-Bénissan A, Dêbare H, Aklikokou K, Dimier-Poisson I, Gbeassor M. 2018. Extracts of *Tectona grandis* and *Vernonia amygdalina* have anti-*Toxoplasma* and pro-inflammatory properties *in vitro*. Parasite. 25, 11.

Deng Y, Wu T, Zhai SQ, Li CH. 2019. Recent progress on anti-*Toxoplasma* drugs discovery: Design, synthesis and screening. Eur J Med Chem. 183, 111711.

Dittmar AJ, Drozda AA, Blader IJ. 2016. Drug repurposing screening identifies novel compounds that effectively inhibit *Toxoplasma gondii* growth. mSphere. 1, e00042-15.

Donald RG, Roos DS. 1998. Gene knock-outs and allelic replacements in *Toxoplasma gondii*: *HXGPRT* as a selectable marker for hit-and-run mutagenesis. Mol Biochem Parasitol. 91, 295-305.

Dubey JP. 1998. Advances in the life cycle of *Toxoplasma gondii*. Int J Parasitol. 28, 1019-1024.

Dubey JP. 2009a. History of the discovery of the life cycle of *Toxoplasma gondii*. Int J Parasitol. 39, 877-882.

Dubey JP. 2009b. Toxoplasmosis in pigs--the last 20 years. Vet Parasitol. 164, 89-103.

Dubey JP, Hill DE, Jones JL, Hightower AW, Kirkland E, Roberts JM, Marcet PL, Lehmann T, Vianna MC, Miska K, Sreekumar C, Kwok OC, Shen SK, Gamble HR. 2005. Prevalence of viable *Toxoplasma gondii* in beef, chicken, and pork from retail meat stores in the United States: risk assessment to consumers. J Parasitol. 91, 1082-1093.

Dunay IR, Gajurel K, Dhakal R, Liesenfeld O, Montoya JG. 2018. Treatment of toxoplasmosis: Historical perspective, animal models, and current clinical practice. Clin Microbiol Rev. 31, e00057-17.

Cowell AN, Winzeler EA. 2019. Advances in omics-based methods to identify novel targets for malaria and other parasitic protozoan infections. Genome Med. 11, 63.

Elmore SA, Jones JL, Conrad PA, Patton S, Lindsay DS, Dubey JP. 2010. *Toxoplasma gondii*: epidemiology, feline clinical aspects, and prevention. Trends Parasitol. 26, 190-196.

El Mouhawass A, Hammoud A, Zoghbi M, Hallit S, Haddad C, El Haddad K, El Khoury S, Tannous J, Obeid S, Halabi MA, Mammari N. 2020. Relationship

between *Toxoplasma gondii* seropositivity and schizophrenia in the Lebanese population: potential implication of genetic polymorphism of MMP-9. BMC Psychiatry. 20, 264.

Esch KJ, Petersen CA. 2013. Transmission and epidemiology of zoonotic protozoal diseases of companion animals. Clin Microbiol Rev. 26, 58-85.

Fleige T, Fischer K, Ferguson DJ, Gross U, Bohne W. 2007. Carbohydrate metabolism in the *Toxoplasma gondii* apicoplast: localization of three glycolytic isoenzymes, the single pyruvate dehydrogenase complex, and a plastid phosphate translocator. Eukaryot Cell. 6, 984-996.

Fleige T, Pfaff N, Gross U, Bohne W. 2008. Localisation of gluconeogenesis and tricarboxylic acid (TCA)-cycle enzymes and first functional analysis of the TCA cycle in *Toxoplasma gondii*. Int J Parasitol. 38, 1121-1132.

Gross P. 1985. Biologic activity of hydroxylamine: a review. Crit Rev Toxicol. 14, 87-99.

Guo H, Gao Y, Jia H, Moumouni PFA, Masatani T, Liu M, Lee SH, Galon EM, Li J, Li Y, Tumwebaze MA, Benedicto B, Xuan X. 2019. Characterization of strain-specific phenotypes associated with knockout of dense granule protein 9 in *Toxoplasma gondii*. Mol Biochem Parasitol. 229, 53-61.

Halonen SK, Weiss LM. 2013. Toxoplasmosis. Handb Clin Neurol. 114, 125-145.

Hortua Triana MA, Márquez-Nogueras KM, Vella SA, Moreno SNJ. 2018. Calcium signaling and the lytic cycle of the Apicomplexan parasite *Toxoplasma gondii*. Biochim Biophys Acta Mol Cell Res. 1865, 1846-1856.

Howe DK, Sibley LD. 1995. *Toxoplasma gondii* comprises three clonal lineages: correlation of parasite genotype with human disease. J Infect Dis. 172, 1561-1566.

Hunter CA, Sibley LD. 2012. Modulation of innate immunity by *Toxoplasma gondii* virulence effectors. Nat Rev Microbiol. 10, 766-778.

Jacot D, Waller RF, Soldati-Favre D, MacPherson DA, MacRae JI. 2016. Apicomplexan energy metabolism: Carbon source promiscuity and the quiescence hyperbole. Trends Parasitol. 32, 56-70.

Jain R, Jordanova R, Müller IB, Wrenger C, Groves MR. 2010. Purification, crystallization and preliminary X-ray analysis of the aspartate aminotransferase of *Plasmodium falciparum*. Acta Crystallogr Sect F Struct Biol Cryst Commun. 66, 409-412.

Johnson SM, Murphy RC, Geiger JA, DeRocher AE, Zhang Z, Ojo KK, Larson ET, Perera BG, Dale EJ, He P, Reid MC, Fox AM, Mueller NR, Merritt EA, Fan E, Parsons M, Van Voorhis WC, Maly DJ. 2012. Development of *Toxoplasma gondii* calcium-dependent protein kinase 1 (*TgCDPK1*) inhibitors with potent anti-toxoplasma activity. J Med Chem. 55, 2416-2426.

Khan A, Dubey JP, Su C, Ajioka JW, Rosenthal BM, Sibley LD. 2011. Genetic analyses of atypical *Toxoplasma gondii* strains reveal a fourth clonal lineage in North America. Int J Parasitol. 41, 645-655.

Kimbita EN, Xuan X, Huang X, Miyazawa T, Fukumoto S, Mishima M, Suzuki H, Sugimoto C, Nagasawa H, Fujisaki K, Suzuki N, Mikami T, Igarashi I. 2001. Serodiagnosis of *Toxoplasma gondii* infection in cats by enzyme-linked immunosorbent assay using recombinant SAG1. Vet Parasitol. 102, 35-44.

Kissinger JC, Gajria B, Li L, Paulsen IT, Roos DS. 2003. ToxoDB: accessing the *Toxoplasma gondii* genome. Nucleic Acids Res. 31, 234-236.

Korsinczky M, Chen N, Kotecka B, Saul A, Rieckmann K, Cheng Q. 2000. Mutations in *Plasmodium falciparum* cytochrome b that are associated with atovaquone resistance are located at a putative drug-binding site. Antimicrob Agents Chemother. 44, 2100-2108.

Kumar S, Stecher G, Tamura K. 2016. MEGA7: Molecular evolutionary genetics analysis version 7.0 for bigger datasets. Mol Biol Evol. 33, 1870-1874.

Lapinskas PJ, Ben-Harari RR. 2019. Perspective on current and emerging drugs in the treatment of acute and chronic toxoplasmosis. Postgrad Med. 131, 589-596.

Leesombun A, Boonmasawai S, Shimoda N, Nishikawa Y. 2016. Effects of extracts from Thai piperaceae plants against infection with *Toxoplasma gondii*. PLoS One. 11, e0156116.

Leesombun A, Iijima M, Umeda K, Kondoh D, Pagmadulam B, Abdou AM, Suzuki Y, Ohba SI, Isshiki K, Kimura T, Kubota Y, Sawa R, Nihei CI, Nishikawa Y. 2020. Metacytofilin is a potent therapeutic drug candidate for toxoplasmosis. J Infect Dis. 221, 766-774.

Liang QL, Sun LX, Elsheikha HM, Cao XZ, Nie LB, Li TT, Li TS, Zhu XQ, Wang JL. 2020. *RHΔgra17Δnpt1* strain of *Toxoplasma gondii* elicits protective immunity against acute, chronic and congenital toxoplasmosis in mice. Microorganisms. 8, 352.

Lima TS, Lodoen MB. 2019. Mechanisms of human innate immune evasion by *Toxoplasma gondii*. Front Cell Infect Microbiol. 9, 103.

Lourido S, Shuman J, Zhang C, Shokat KM, Hui R, Sibley LD. 2010. Calcium-dependent protein kinase 1 is an essential regulator of exocytosis in *Toxoplasma*. Nature. 465, 359-362.

Lourido S, Tang K, Sibley LD. 2012. Distinct signalling pathways control *Toxoplasma* egress and host-cell invasion. EMBO J. 31, 4524-4534.

MacRae JI, Sheiner L, Nahid A, Tonkin C, Striepen B, McConville MJ. 2012. Mitochondrial metabolism of glucose and glutamine is required for intracellular growth of *Toxoplasma gondii*. Cell Host Microbe. 12, 682-692.

Mahmoud ME, Ui F, Salman D, Nishimura M, Nishikawa Y. 2015. Mechanisms of interferon-beta-induced inhibition of *Toxoplasma gondii* growth in murine macrophages and embryonic fibroblasts: role of immunity-related GTPase M1. Cell Microbiol. 17, 1069-1083.

Manchola NC, Silber AM, Nowicki C. 2018. The non-canonical substrates of trypanosoma cruzi tyrosine and aspartate aminotransferases: Branched-chain amino acids. J Eukaryot Microbioly. 65, 70-76.

Marković-Housley Z, Schirmer T, Hohenester E, Khomutov AR, Khomutov RM, Karpeisky MY, Sandmeier E, Christen P, Jansonius JN. 1996. Crystal structures and solution studies of oxime adducts of mitochondrial aspartate aminotransferase. Eur J Biochem. 236, 1025-1032.

Masatani T, Matsuo T, Tanaka T, Terkawi MA, Lee EG, Goo YK, Aboge GO, Yamagishi J, Hayashi K, Kameyama K, Cao S, Nishikawa Y, Xuan X. 2013. *Tg*GRA23, a novel *Toxoplasma gondii* dense granule protein associated with the parasitophorous vacuole membrane and intravacuolar network. Parasitol Int. 62, 372-379.

Matsubayashi H, Akao S. 1963. Morphological studies of the development of the *Toxoplasma* cyst. Am J Trop Med Hyg. 12, 321-333.

McFarland MM, Zach SJ, Wang X, Potluri LP, Neville AJ, Vennerstrom JL, Davis PH. 2016. Review of experimental compounds demonstrating anti-*Toxoplasma* activity. Antimicrob Agents Chemother. 60, 7017-7034.

Montazeri M, Mehrzadi S, Sharif M, Sarvi S, Shahdin S, Daryani A. 2018a. Activities of anti-*Toxoplasma* drugs and compounds against tissue cysts in the last three decades (1987 to 2017), a systematic review. Parasitol Res. 117, 3045-3057.

Montazeri M, Mehrzadi S, Sharif M, Sarvi S, Tanzifi A, Aghayan SA, Daryani A. 2018b. Drug resistance in *Toxoplasma gondii*. Front Microbiol. 9, 2587.

Montazeri M, Sharif M, Sarvi S, Mehrzadi S, Ahmadpour E, Daryani A. 2017. A systematic review of *in vitro* and *in vivo* activities of anti-*Toxoplasma* drugs and compounds (2006-2016). Front Microbiol. 8, 25.

Montoya JG, Liesenfeld O. 2004. Toxoplasmosis. Lancet. 363, 1965-1976.

Mordue DG, Monroy F, La Regina M, Dinarello CA, Sibley LD. 2001. Acute toxoplasmosis leads to lethal overproduction of Th1 cytokines. J Immunol. 167, 4574-4584.

Müller J, Hemphill A. 2016. Drug target identification in protozoan parasites. Expert Opin Drug Discov. 11, 815-824.

Nishikawa Y, Xuenan X, Makala L, Vielemeyer O, Joiner KA, Nagasawa H. 2003. Characterisation of *Toxoplasma gondii* engineered to express mouse interferon-gamma. Int J Parasitol. 33, 1525-1535.

Nishikawa Y, Zhang H, Ibrahim HM, Ui F, Ogiso A, Xuan X. 2008. Construction of *Toxoplasma gondii* bradyzoite expressing the green fluorescent protein. Parasitol Int. 57, 219-222.

Nitzsche R, Zagoriy V, Lucius R, Gupta N. 2016. Metabolic cooperation of glucose and glutamine is essential for the lytic cycle of obligate intracellular parasite *Toxoplasma gondii*. J Biol Chem. 291, 126-141.

Oppenheim RD, Creek DJ, Macrae JI, Modrzynska KK, Pino P, Limenitakis J, Polonais V, Seeber F, Barrett MP, Billker O, McConville MJ, Soldati-Favre D. 2014. BCKDH: the missing link in apicomplexan mitochondrial metabolism is required for full virulence of *Toxoplasma gondii* and *Plasmodium berghei*. PLoS Pathog. 10, e1004263.

Pifer R, Yarovinsky F. 2011. Innate responses to *Toxoplasma gondii* in mice and humans. Trends Parasitol. 27, 388-393.

Radke JB, Carey KL, Shaw S, Metkar SR, Mulrooney C, Gale JP, Bittker JA, Hilgraf R, Comer E, Schreiber SL, Virgin HW, Perez JR, Sibley LD. 2018. High throughput screen identifies interferon γ-dependent inhibitors of *Toxoplasma gondii* growth. ACS Infect Dis. 4, 1499-1507.

Reynolds MG, Oh J, Roos DS. 2001. *In vitro* generation of novel pyrimethamine resistance mutations in the *Toxoplasma gondii* dihydrofolate reductase. Antimicrob Agents Chemother. 45, 1271-1277.

Saadatnia G, Golkar M. 2012. A review on human toxoplasmosis. Scand J Infect Dis. 44, 805-814.

Salin NH, Noordin R, Al-Najjar BO, Kamarulzaman EE, Yunus MH, Karim IZA, Nasim NNM, Zakaria II, Wahab HA. 2020. Identification of potential dual-

targets anti-*Toxoplasma gondii* compounds through structure-based virtual screening and in-vitro studies. PLoS One. 15, e0225232.

Sarojini G, Oliver DJ. 1985. Inhibition of glycine oxidation by carboxymethoxylamine, methoxylamine, and acethydrazide. Plant Physiol. 77, 786-789.

Sasai M, Pradipta A, Yamamoto M. 2018. Host immune responses to *Toxoplasma gondii*. Int Immunol. 30, 113-119.

Sasai M, Yamamoto M. 2019. Innate, adaptive, and cell-autonomous immunity against *Toxoplasma gondii* infection. Exp Mol Med. 51, 1-10.

Sayles PC, Gibson GW, Johnson LL. 2000. B cells are essential for vaccination-induced resistance to virulent *Toxoplasma gondii*. Infect Immun. 68, 1026-1033.

Scheele S, Geiger JA, DeRocher AE, Choi R, Smith TR, Hulverson MA, Vidadala RSR, Barrett LK, Maly DJ, Merritt EA, Ojo KK, Van Voorhis WC, Parsons M. 2018. *Toxoplasma* calcium-dependent protein kinase 1 Inhibitors: Probing activity and resistance using cellular thermal shift assays. Antimicrob Agents Chemother. 62, e00051-18.

Shen B, Brown K, Long S, Sibley LD. 2017. Development of CRISPR/Cas9 for efficient genome editing in *Toxoplasma gondii*. Methods Mol Biol. 1498, 79-103.

Shen B, Sibley LD. 2014. *Toxoplasma* aldolase is required for metabolism but dispensable for host-cell invasion. Proc Natl Acad Sci USA. 111, 3567-3572.

Shukla A, Olszewski KL, Llinás M, Rommereim LM, Fox BA, Bzik DJ, Xia D, Wastling J, Beiting D, Roos DS, Shanmugam D. 2018. Glycolysis is important

for optimal asexual growth and formation of mature tissue cysts by *Toxoplasma gondii*. Int J Parasitol. 48, 955-968.

Sibley LD, Ajioka JW. 2008. Population structure of *Toxoplasma gondii*: clonal expansion driven by infrequent recombination and selective sweeps. Annu Rev Microbiol. 62, 329-351.

Siqueira-Neto JL, Debnath A, McCall LI, Bernatchez JA, Ndao M, Reed SL, Rosenthal PJ. 2018. Cysteine proteases in protozoan parasites. PLoS Negl Trop Dis. 12, e0006512.

Soete M, Fortier B, Camus D, Dubremetz JF. 1993. *Toxoplasma gondii*: kinetics of bradyzoite-tachyzoite interconversion in vitro. Exp Parasitol. 76, 259-264.

Soldati D, Boothroyd JC. 1993. Transient transfection and expression in the obligate intracellular parasite *Toxoplasma gondii*. Science. 260, 349-352.

Spellberg B, Edwards JE, Jr. 2001. Type 1/Type 2 immunity in infectious diseases. Clin Infect Dis. 32, 76-102.

Suzuki Y, Orellana MA, Schreiber RD, Remington JS. 1988. Interferon-gamma: the major mediator of resistance against *Toxoplasma gondii*. Science. 240, 516-518.

Uddin T, McFadden GI, Goodman CD. 2018. Validation of putative apicoplast-targeting drugs using a chemical supplementation assay in cultured human malaria parasites. Antimicrob Agents Chemother. 62, e01161-17.

VanWormer E, Fritz H, Shapiro K, Mazet JA, Conrad PA. 2013. Molecules to modeling: *Toxoplasma gondii* oocysts at the human-animal-environment interface. Comp Immunol Microbiol Infect Di. 36, 217-231.

Wang JL, Elsheikha HM, Li TT, He JJ, Bai MJ, Liang QL, Zhu XQ, Cong W. 2019a. Efficacy of antiretroviral compounds against *Toxoplasma gondii in vitro*. Int J Antimicrob Agents. 54, 814-819.

Wang M, Cao S, Du N, Fu J, Li Z, Jia H, Song M. 2017b. The moving junction protein RON4, although not critical, facilitates host cell invasion and stabilizes MJ members. Parasitology. 144, 1490-1497.

Wei HX, Wei SS, Lindsay DS, Peng HJ. 2015. A systematic review and meta-analysis of the efficacy of Anti-*Toxoplasma gondii* medicines in humans. PLoS One. 10, e0138204.

Weiss LM, Dubey JP. 2009. Toxoplasmosis: A history of clinical observations. Int J Parasitol. 39, 895-901.

Wrenger C, Müller IB, Schifferdecker AJ, Jain R, Jordanova R, Groves MR. 2011. Specific inhibition of the aspartate aminotransferase of *Plasmodium falciparum*. J Mol Biol. 405, 956-971.

Wrenger C, Muller IB, Silber AM, Jordanova R, Lamzin VS, Groves MR. 2012. Aspartate aminotransferase: bridging carbohydrate and energy metabolism in *Plasmodium falciparum*. Curr Drug Metab. 13, 332-336.

Wong ZS, Borrelli SLS, Coyne CC, Boyle JP. 2020. Cell type- and species-specific host responses to *Toxoplasma gondii* and its near relatives. Int J Parasitol. 50, 423-431.

Xia N, Yang J, Ye S, Zhang L, Zhou Y, Zhao J, David Sibley L, Shen B. 2018a. Functional analysis of *Toxoplasma* lactate dehydrogenases suggests critical roles of lactate fermentation for parasite growth in vivo. Cell Microbiol. 20, 10.

Xia N, Ye S, Liang X, Chen P, Zhou Y, Fang R, Zhao J, Gupta N, Yang S, Yuan J, Shen B. 2019. Pyruvate homeostasis as a determinant of parasite growth and metabolic plasticity in *Toxoplasma gondii*. mBio. 10, e00898-19.

Xia N, Zhou T, Liang X, Ye S, Zhao P, Yang J, Zhou Y, Zhao J, Shen B. 2018b. A lactate fermentation mutant of *Toxoplasma* stimulates protective immunity against acute and chronic toxoplasmosis. Front Immunol. 9, 1814.

Xie SC, Dick LR, Gould A, Brand S, Tilley L. 2019. The proteasome as a target for protozoan parasites. Expert Opin Ther Targets. 23, 903-914.

Yang J, Wang L, Xu D, Tang D, Li S, Du F, Wang L, Zhao J, Fang R. 2018. Risk assessment of etanercept in mice chronically infected with *Toxoplasma gondii*. Front Microbiol. 9, 2822.

Yang WB, Wang JL, Gui Q, Zou Y, Chen K, Liu Q, Liang QL, Zhu XQ, Zhou DH. 2019. Immunization with a live-attenuated *RH:ΔNPT1* strain of *Toxoplasma gondii* induces strong protective immunity against toxoplasmosis in mice. Front Microbiol. 10, 1875.

Yarovinsky F. 2014. Innate immunity to *Toxoplasma gondii* infection. Nat Rev Immunol. 14, 109-121.

Yarovinsky F, Sher A. 2006. Toll-like receptor recognition of *Toxoplasma gondii*. Int J Parasitol. 36, 255-259.

Zheng J, Jia H, Zheng Y. 2015. Knockout of leucine aminopeptidase in *Toxoplasma gondii* using CRISPR/Cas9. Int J Parasitol. 45, 141-148.